remote sensing

MDPI

Article

Ground Electric Field, Atmospheric Weather and Electric Grid Variations in Northeast Greece Influenced by the March 2012 Solar Activity and the Moderate to Intense Geomagnetic Storms

Georgios Anagnostopoulos [1,*], Anastasios Karkanis [1], Athanasios Kampatagis [2], Panagiotis Marhavilas [3], Sofia-Anna Menesidou [4], Dimitrios Efthymiadis [1], Stefanos Keskinis [5], Dimitar Ouzounov [6], Nick Hatzigeorgiu [7] and Michael Danikas [1]

[1] Department of Electrical and Computer Engineering, Democritus University of Thrace (DUTH), 67100 Xanthi, Greece; ankark@ee.duth.gr (A.K.); deythym@ee.duth.gr (D.E.); mdanikas@ee.duth.gr (M.D.)
[2] Thermal Power Plant of Operation Department, TPP, 69132 Komotini, Greece; a.kampatagis@dei.gr
[3] Department of Production and Management Engineering, Democritus University of Thrace, Vas. Sofias 12 St., 67132 Xanthi, Greece; marhavil@pme.duth.gr
[4] R&D Department, Ubitech Ltd., 11632 Athens, Greece; smenesid@ee.duth.gr
[5] Hellenic Electricity Distribution Network Operator, Network Major Installations Department, 18547 Athens, Greece; s.keskinis@deddie.gr
[6] Institute for Earth, Computing, Human and Observing (Institute for ECHO), Chapman University, Orange, CA 92866, USA; ouzounov@chapman.edu
[7] Space Sciences Lab, University of California, Berkeley, CA 94720, USA; nikos@berkeley.edu
* Correspondence: ganagno@ee.duth.gr; Tel.: +30-25410-20486

Abstract: In a recent paper, we extended a previous study on the solar solar influence to the generation of the March 2012 heatwave in the northeastern USA. In the present study we check the possible relationship of solar activity with the early March 2012 bad weather in northeast Thrace, Greece. To this end, we examined data from various remote sensing instrumentation monitoring the Sun (SDO satellite), Interplanetary space (ACE satellite), the Earth's magnetosphere (Earth-based measurements, NOAA-19 satellite), the top of the clouds (Terra and Aqua satellites), and the near ground atmosphere. Our comparative data analysis suggests that: (i) the winter-like weather (rainfall, fast winds, decreased temperature) in Thrace started on 6 March 2012, the same day as the heatwave started in USA, (ii) during the March 2012 winter-like event in Thrace (6–15 March), the ACE satellite recorded enhanced fluxes of solar energetic particles (SEPs), while SOHO and PAMELA recorded solar protons at very high energies (>500 MeV), (iii) Between 3–31 March, the temperature in Alexandoupoli and the ACE/EPAM solar high energy (1.88–4.70 MeV) proton flux were strongly anticorelated (r = −0.75, p = 0.5). (iv) Thrace experienced particularly intense cyclonic circulation, during periods of magnetic storms on 8–10 and 12–13 March, which occurred after the arrival at ACE of two interplanetary shock waves, on March 8 and March 11, respectively, (v) at the beginning of the two above mentioned periods large atmospheric electric fields were recorded, with values ranging between ~−2000 V/m and ~1800 V/m on 8 March, (vi) the winter-like weather on 8–10 March 2012 occurred after the detection of the main SEP event related with a coronal mass ejection released in interplanetary space as a result of intense solar flare activity observed by SDO on 7 March 2012, (vi) the 8–10 March weather was related with a deep drop of ~63 °C in the cloud top temperature measured by MODIS/Terra, which favors strong precipitation. Finally, we analyzed data from the electric power network in Thrace (~41°N) and we found, for the first time sudden voltage changes of ~3.5 kV in the electric grid in Greece, during the decay phase of the March 2012 storm series. We discuss the winter-like March 2012 event in Thrace regarding the influence of solar cosmic rays on the low troposphere mediated by positive North Atlantic Oscillation (NAO). Finally, we infer that the novel finding of the geomagnetic effects on the electric power grid in Thrace may open a new window into space weather applications research.

Keywords: extreme weather events; solar-terrestrial relationships; GICs; SEPs; March 2012 events; NAO effects; Mediterranean cyclones; cloud top temperature; climate change

check for updates

Citation: Anagnostopoulos, G.; Karkanis, A.; Kampatagis, A.; Marhavilas, P.; Menesidou, S.-A.; Efthymiadis, D.; Keskinis, S.; Ouzounov, D.; Hatzigeorgiu, N.; Danikas, M. Ground Electric Field, Atmospheric Weather and Electric Grid Variations in Northeast Greece Influenced by the March 2012 Solar Activity and the Moderate to Intense Geomagnetic Storms. *Remote Sens.* **2024**, *16*, 998. https://doi.org/10.3390/rs16060998

Academic Editor: Mike Wolff

Received: 18 December 2023
Revised: 14 February 2024
Accepted: 16 February 2024
Published: 12 March 2024

1. Introduction

1.1. Solar Activity and the Subsequent Space Weather as Drivers of Variations in Earth's Atmosphere

The solar influence on the Earth's climate has been studied for a long time. The historic Maunder minimum (MM), between AD 1650 and 1715 [1] and the Medieval warm period, around 1000 AD [2] are well-known events at least in the space and atmospheric physics communities. During the space era, Earth-based and satellite measurements have shown that interplanetary coronal mass injections (ICMEs) affect the whole atmosphere up to low altitudes (~2000 m above sea level) [3].

The Sun is the principal energy source in the atmosphere and biosphere. The Sun affects the earth's environment via electromagnetic radiation, solar energetic particle (SEP) events and solar wind plasma. The crucial question we address in relative science communities is whether solar activity may contribute to some extent to the increased number of dangerous extreme atmospheric events.

In a previous case study, we considered for the first time, the possible solar influence on extreme events, by comparing space weather and atmospheric parameters during the March 2012 heatwave (M2012HW) in the northeast USA [4]. We found strong evidence that both the M2012HW and the historic March 1910 heatwave were most probably caused by solar activity-induced effects on the Earth's magnetosphere and atmosphere.

Global warming is considered to be a manifestation of the increased frequency of extreme events in our times [5,6]. A CarbonBrief report entitled "Attributing Extreme Weather to Climate Change" suggests that human activity has been raising the risk of some kind of extreme weather, in particular, heatwaves [7]. Many authors interpret this statement in the sense that climate change should not be considered the sole cause of each one of the extreme weather events. According to these authors, some natural variations can also trigger extreme events [8–10]. Ref. [7] claim that no reliable discernible influence owing to human activity has been found in ~10% of the extreme weather events and trends that they studied, while in a further 11% of the extreme weather events no reliable conclusion could be reached. Connolly et al., in a recent review paper entitled "How Much Has the Sun Influenced Northern Hemisphere Temperature Trends? An Ongoing Debate", claimed that the debate on "anthropogenic versus solar influence" has not yet reached a consensus, and further data analysis and theoretical discussion is needed [11].

In this paper, we continued our previous studies on solar-terrestrial relationships by investigating the origin of the March 2012 heatwave in the northeast USA. We examine data from various remote sensing sources: the Sun (SDO satellite), the Interplanetary Space (ACE satellite), the Earth's magnetosphere (Earth-based measurements, NOAA-19 satellite), the top of the clouds (Terra and Aqua satellites) and the near ground atmosphere. Ultimately, we check the possible relationship of solar activity with the early March 2012 bad weather in northeast Thrace, Greece. Our comparative data analysis suggests: (i) the winter-like weather in Thrace started on the same day as the heatwave started in the USA, (ii) during March 2012, the ACE satellite recorded enhanced flux of SEPs, while the high energy (>~2 MeV) proton flux showed an anti-correlation with the temperature in Thrace (Alexandroupoli), (iii) Thrace experienced particularly intense cyclonic circulation, with intensified events during two periods of magnetic storms (8–10 and 12–13 March), (iv) the winter-like period occurred after the detection of the main SEP event related with the main ICME, (v) the weather in Thrace was related with a deep drop of ~63 °C in the cloud top temperature measured by MODIS/Terra, (vi) SOHO and PAMELA recorded very high energy (>500 MeV) solar proton streams and large atmospheric electric field fluctuations recorded (with values reaching ~−2000 V/m) at the beginning of the two above mentioned magnetic storms. Finally, we present high-time resolution (within 1 s) data from Thrace's power network (~41°N). We discuss the winter-like March 2012 event in Thrace regarding the influence of solar cosmic rays on the low troposphere mediated by positive NAO. In the Discussion, we suggest that the novel methodology we used of continuous monitoring the geomagnetic effects on the electric power grid may open new opportunities for space weather applications research. Our data analysis provides good evidence of the influence of the unusual March 2012 solar and interplanetary space conditions on extreme events in Thrace, Greece at middle latitudes (~41°N).

1.2. Solar Activity

One of the most important solar phenomena is coronal mass ejection (CME) [12]. Once a CME escapes from the Sun, it propagates in interplanetary space and reaches the Earth's orbit at velocities ranging from ~350 km/s to ~2000 km/s. The time it takes a CME to arrive from the Sun to the Earth is about two days, although there are significant variations as far as the duration time is concerned [13]. A CME expanding in the interplanetary space can create a shock wave (SW) accelerating particles to high (GeV) energies, which are observed as large particle fluxes around the SW, and are known as solar energetic particle (SEP) events. Whenever a CME erupts on the side of the Sun facing Earth, and the Earth's orbit intersects the path of the CME cloud, spectacular and sometimes hazardous effects are observed [5,6]. An ICME reaching the Earth's magnetosphere induces geomagnetic disturbance, a magnetic storm, due to solar wind plasma pressure and southward interplanetary magnetic field (IMF) interactions with the magnetosphere/bow shock. The most spectacular effect of ICMEs is the aurorae, which appear as curtains, rays and spirals in dynamic variations in the sky, predominantly seen in high-latitude regions.

The corotating interaction regions (CIR) consist a second type of solar activity that influences the Earth's enviroement. In this case, the fast solar wind catches up with upstream slow solar wind and a compressive region is formed at the interface of the fast and the slow streams. These structures reappear with the solar rotation period ($\sim$27 days). When these coronal hole-associated fast solar wind streams are long lasting, they lead to the formation of CIRs.

Both ICMEs and CIRs are drivers of geomagnetic storms. Furthermore, Solar activity (ICMEs and CIRs) causes various types of physical processes in Earth's magnetosphere [13–16], ionosphere [17,18], atmosphere [4,19,20], lithosphere [21–23], biosphere [24–27] and technosphere [28–30].

1.3. Solar Energetic Particles and Tropospheric Variations

The research on solar–terrestrial relationships has emphasized solar cycle ($\approx$11-year periodicity) climate trends so far and has concentrated on stratospheric changes, polar variations, cloudy and sea/surface temperatures [19,31]. Furthermore, it is accepted that solar activity affects both long-term (climate) and short-term (weather) variation [3,11,31–37].

Short-term meteorological responses to solar variable activity have been reported since the beginning of the space era [33]. For instance, Schuurmans [33] reported changes at the tropopause within 12 h after strong solar flares and other tropospheric effects 2–4 days after the flares. Furthermore, Pudovkin and Raspopov [38] and Pudovkin and Babushkina [39], provided significant evidence that the leading cause of weather variations in the lower atmosphere are solar and galactic cosmic ray radiation.

Avakyan et al. [3] studied the meteorological variations at low heights during the Halloween October 2003 solar events and they observed a temperature increase after large magnetic storms (Kp > 5) in 84% of the cases studied at an altitude of 2100 m (at the mountain meteorological observatory near Kislovodsk). Moreover, strong electric field fluctuations were reported after the 2003 Halloween events in Kamchatka and many other researchers reported various other atmospheric reflections following the October 2003 solar events [40,41]. In addition galactic cosmic rays appear to play a significant part in climate and weather [42–45].

In conclusion, various studies indicate that after a solar flare, tropospheric variations can occur with in 2–4 days, i.e., the time required for a CME released into interplanetary space to reach our planet.

1.4. CME-Related Geomagnetically Induced Electric Fields and Currents on the Ground

During an ICME-induced magnetic storm the geomagnetic field changes. The induced electric field also creates currents in man-made conductor systems, such as telecommunication cables, electric power networks, oil and gas pipelines, and railway equipment; these currents have been called "geomagnetically induced currents" or GIC [28,46]. GICs are related with surface voltages with values between ~1 V/km and ~5 V/km, with maximum values of ~20 V/km [47].

The GICs are generally of the order of tens to hundreds of amperes. These quasi-DC currents are small compared to the normal AC flowing in the network, but they can induce an enormous impact on the operation of transformers. GIC levels of only 1–10 A can initiate magnetic core saturation in a transformer. The geomagnetic variations are slow (#mHz) compared to the frequency used in electric power transmission (50 or 60 Hz). Therefore when a GIC flows through a transformer, it acts as a DC current. Then, as a result, highly distorted transformer currents are injected into the electric power network [48].

Studies on the effects of solar eruptions on the Earth's electric field and, consequently, in electric power grids, began relatively recently, after a CME in 1979 [30]. The most famous GIC-induced electric failure occurred in the Hydro-Quebec power system in 1989 [47–50]. Although GICs usually appear at high latitudes, a large ICME may cause GICs at middle and even low latitudes. During the famous 2003 Halloween events, the magnetic variations produced an intense electric field on the ground across the UK. After that event, the GICs raised significant concern within the power industry and government [51].

Liu et al. [14] attempted to identify the responses to space disturbances in low latitude China during a modest magnetic storm on 14 July 2012. They inferred that some transformers had more or less responses to moderate storms depending on the type of transformer and the grid, under similar geographical conditions (i.e., latitude, ground resistivity) [52].

As GICs increase, the level of saturation of an electric transformer core and its impact on the operation of the power network increases. For large storms, the spatial coverage of the magnetic disturbance is large and a large number of transformers can be simultaneously saturated, which can rapidly escalate into a network-wide voltage collapse. In addition, individual transformers may be damaged from overheating due to the unusual operational mode, resulting in long-term outages to critical transformers in the network. Damage to these assets can slow the complete restoration of power network operations [48]. Space scientists have strengthened their research in space weather prediction so that industry and states can avoid catastrophic effects in electric power systems.

In this study we will present results from the electric grid in Thrace, northeast Greece, at ~40°N, revealing voltage disturbances during the March 2012 series of magnetic storms. This is the first (case) study focusing only on high time resolution (1 s) sudden voltage changes (SVCs) in an electric power grid. The new methodology of studying a plethora of SVCs (28 events on March 2012) is considered as a direct manifestation of magnetic storm influencing a power system and hopefully could be used in space-related power network failure forecasting research, as an independent index, in parallel to the GICs.

1.5. Vertical Atmospheric Electric Field Ez near the Ground during Magnetic Storms

The atmospheric electric field (AEF) Ez is the field exists in the atmosphere due to the ground and ionosphere, which are negatively and positively charged, respectively. The AEF is formed by the potential difference of 250 kV between the ionosphere and the Earth's surface [53] and is directed vertically toward the ground, under fair weather conditions. Globally, the Ez value is approximately 100 V/m–200 V/m [54,55]. The variability in the atmospheric electric field is strongly dependent on a combination of conditions and it is divided into fair-weather AEF and disturbed-weather AEF.

The vertically orientated AEF Ez can be affected by weather conditions, soil morphology and solar activities [56]. The AEF can also be affected by thunderstorms [57–59], cloudiness [60], geomagnetic activities [61], solar activities [62,63] and air pollution [64,65].

Also, in some places the environmental and meteorological differences can affect the AEF [66–70]. Furthermore, the AEF is influenced by earthquakes [71–74].

Significant work has recently been based on disturbed AEF Ez's relationship with space weather. Among others, Kleimenova et al. presented the effect of 14 magnetic storm main phases in daytime mid-latitude variations in the vertical component *Ez* of the atmospheric electric field, without local geomagnetic disturbances [75]. They reported, under conditions of fair weather, considerable (~100–300 V/ m) decreases in *Ez* values at Swidermidlatitude Poland observatory (47.8°N), during the onset of a substorm in nighttime auroral latitudes (College observatory). They inferred that an increase in the precipitation of energetic electrons into the nighttime auroral ionosphere, can result in considerable disturbances in the midlatitude AEF.

Strong electric field fluctuations were reported, among others, by Smirnov et al. after the 2003 Halloween events in Kamchatka [40]. Michnowski et al. compared measurements made at ground level in both the Arctic (S. Siedlecki Polish Polar Station Hornsund, Spitsbergen, Svalbard, Norway) and at mid-latitudes (Swider, S. Kalinowski Geophysical Observatory, Świder, Poland) [76]. They inferred that the solar wind changes produce measurable effects on ground-level *Ez* and *Jz* at middle latitudes, dependent on the strength of the ICME-induced magnetic storms. These authors claimed that the almost-simultaneous detection of solar wind parameter changes, magnetic storms and variations in the *Ez*/*Jz* confirms their physical relationship.

2. Instruments and Data

The Solar Dynamics Observatory (SDO) was designed to understand the Sun's variability and its impacts on Earth. It was launched on 11 February 2010 (https://sdo.gsfc.nasa.gov/; accessed on 20 September 2023). The mission aim is to advance the predictive capability of solar influence on Earth's humanity and humanity's technological systems [77]. The SDO mission includes three scientific investigations: the Atmospheric Imaging Assembly (AIA), the Extreme Ultraviolet Variability Experiment (EVE), and the Helioseismic and Magnetic Imager (HMI). Here we use measurements from the Atmospheric Imaging Assembly (AIA) telescope taking images from the Sun every 10 s. This study examines the images in the passband of 4500 A° and 171 A° (https://helioviewer.org; accessed on 20 September 2023).

The space weather research is based on measurements obtained by the NASA Advanced Composition Explorer (ACE) satellite [78] (http://www.srl.caltech.edu/ACE/, accessed on 27 May 2022). ACE circulates the L1 Lagrangian point (Figure 1), at a distance of ≈220 R_E from the Earth (Figure 1; R_E is the length of the Earth's radius). (https://www.swpc.noaa.gov/products/ace-real-time-solar-wind, accessed on 27 May 2022). The present paper presents energetic particle data from the EPAM experiment [4].

Terra is in a circular sun-synchronous polar orbit completing a revolution every 99 min. The Terra satellite explores the connections between Earth's atmosphere, land, snow and ice, ocean, and energy balance to understand Earth's climate and climate change and to map the impact of human activity and natural disasters on communities and ecosystems. It moves at an altitude of ~700 km with an inclination of 98.50 (https://terra.nasa.gov; accessed on 20 September 2023). Aqua is also in a circular sun-synchronous polar orbit with a period of 98.8 min, an altitude of ~700 km, and an inclination of 98.2 (https://aqua.nasa.gov/content/about-aqua; accessed on 20 September 2023) [79,80]. The Moderate-Resolution Imaging Spectroradiometer (MODIS) is a key instrument aboard NASA's Terra and Aqua satellites to improve understanding of global atmospheric dynamics and processes occurring on Earth and in its environment [81].

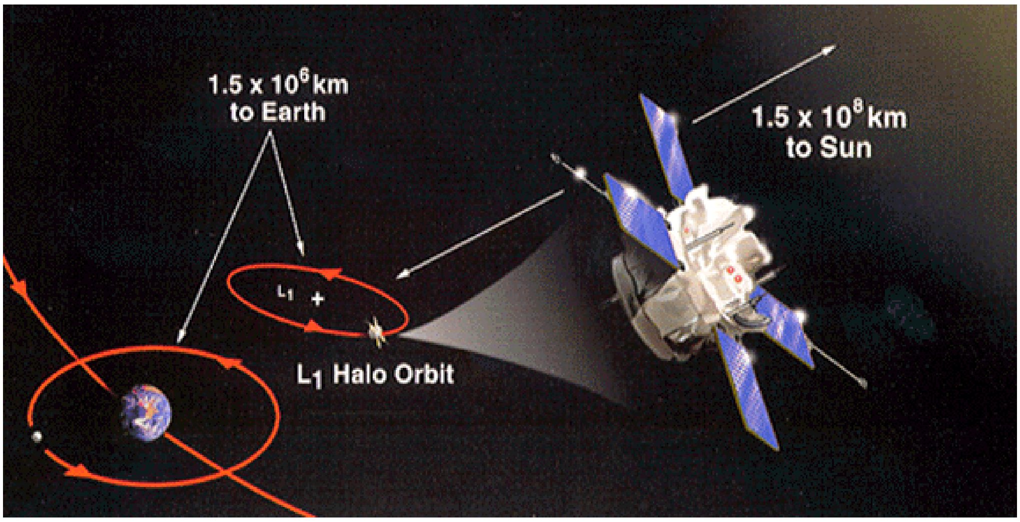

Figure 1. ACE circulating, around the L_1 Lagrangian point. The L_1 Earth-Sun gravitational equilibrium lies at a distance of ~220 R_E. Real-time data from ACE are used to predict and improve forecasts and warnings of geomagnetic storms and other important phenomena at or near Earth.

NOAA 19 is the fifth in a series of five (Polar Operational Environmental Satellites) (POESs) circling at ~850 km above Earth with a period of ~100 min.

The data used in our study for revealing variations in the high voltage 150 kV transmission network come from the SCADA system of the Thermal Power Plant of Komotini, which is located in Thrace, Northern Greece [82].

3. Data Analysis Results

3.1. March 2012 Extreme Events

In a recent paper, we provided significant evidence that the March 2012 heat wave in the northeast USA was affected by solar activity [4]. The conclusion was based on the comparison (i) of observations in the near-Earth interplanetary space (ACE satellite at the Lagrangian L1 point between the Sun and the Earth) and on Earth's ground, and (ii) of the March 2012 heatwave with the March 1910 heatwave, which occurred before the Greenhouse Gases (GHG) effect and is understood as a non-anthropogenic, a natural event. The conclusion was supported by an elaborate discussion of a CME–related heat wave in March 2012.

The March 2012 heatwave was not a local, American extreme weather event. March 2012 is also known for extreme meteorological weather events occurring all over the globe. Here we examine the atmospheric weather in southeast Europe after a geoeffective coronal mass ejection incident. We incorporate remote sensing data revealing the spatio-temporal variations on the solar disk (SDO satellite) and the top of the clouds (Terra satellite). The space weather, which affects (and to some extent predicts) the large-scale electromagnetic environment of Earth (magnetosphere, ionosphere, atmosphere) is examined by using the ACE observations at the Lagrangian L1 point between the Sun and the Earth, as in our study of the March 2012 heat wave [4]. In [4] we inferred that the unusual space, magnetospheric, ionospheric and atmospheric events in March 2012 started after the solar active region (AR) 11429 appeared on 5 March. Figure 2 shows images from the solar corona, obtained by the AIA telescope onboard SDO on 7 March. Figure 2a clearly shows the AR11429 at 00.00:08 UT in the passband of 4500 A° on the northeast side of the disk. The AIA telescope on the SDO satellite recorded a barrage of two X-class flares in rapid succession. The first flare was an X5.4 from N18° E31°, starting at 00:02 UT on 7 March and peaking at 00:24 UT, while the second, at N15° E26°, was an X1.4 flare, which started at 01:05 UT and peaked at 01:14 UT. We note that an X2 flare is twice the strength of an X1 flare, an X3 flare is three times as powerful as an X1, etc., which suggests that X5.4 was a highly intense solar flare. Image a clearly shows the active region (at 00.00:08 UT), which was responsible for the intense ICMEs strongly affected the Earth's magnetosphere and atmosphere in March 2012. Images b and c were obtained just before (00.04:24 UT) and after (00.24:48 UT) the X5.4 flare (peaking at 00:24 UT) on 7 March. The two images (b and c) were obtained by AIA in the passband of 171 A° just before the X5.4 flare (peaking at 00:24 UT). The comparison of the two images reasonably suggests the difference in brightness after 00:24 UT. Both flares, X5.4 (F1) and X1.4 (F2), were accompanied by two ultra-fast (>2000 km/s) CMEs and highly disturbed the Earth's magnetosphere.

In Figure 3 we combine space and atmospheric weather data temporally related to the intense solar flares and the subsequent eruption of the two CMEs in March 2012; the two upper panels, a and b, provide information on the atmospheric weather in Alexadroupoli, in particular: temperature (panel a) and precipitation (panel b).

(**a**)

(**b**)

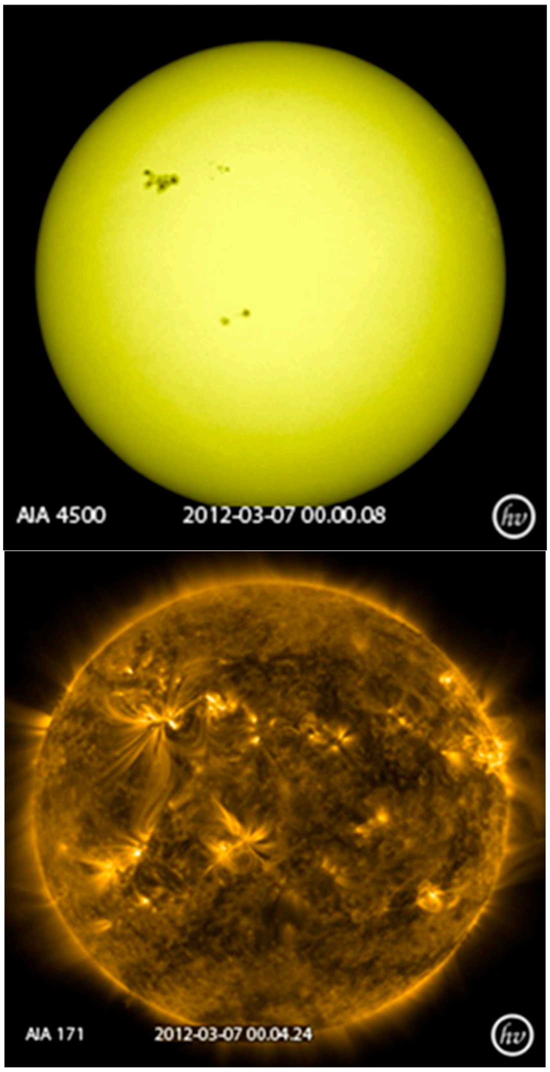

Figure 2. *Cont.*

(**c**)

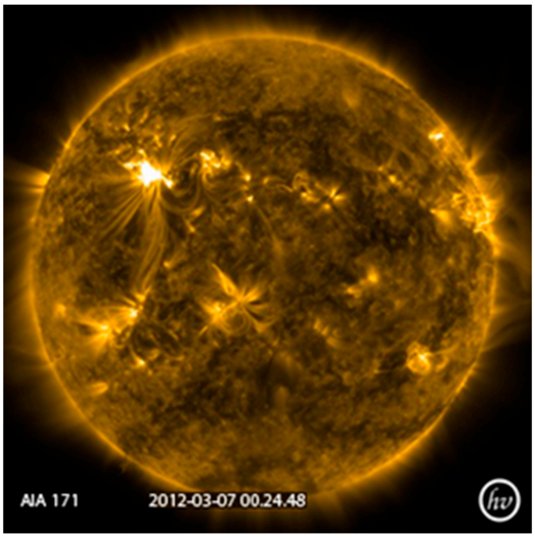

Figure 2. Images of the Sun obtained by the telescope Atmospheric Imaging Assembly (AIA) onboard the Solar Dynamics Observatory (SDO) satellite on 7 March 2012 in the passband of 4500 A° (**a**) and 171 A° (**b**,**c**). Image a clearly shows the active region (at 00.00:08 UT), which was responsible for the intense ICMEs strongly affected the Earth's magnetosphere and atmosphere in March 2012. (**b**,**c**) were obtained just before (00.04:24 UT) and after (00.24:48 UT) the X5.4 flare (00:24 UT) on 7 March.

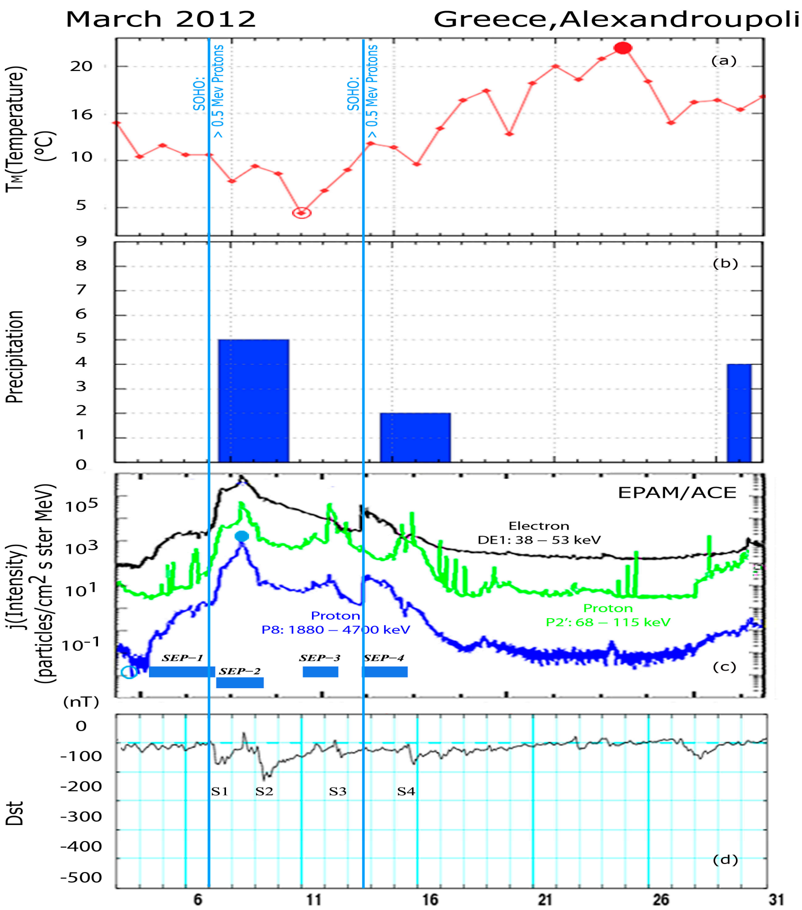

Figure 3. *Cont.*

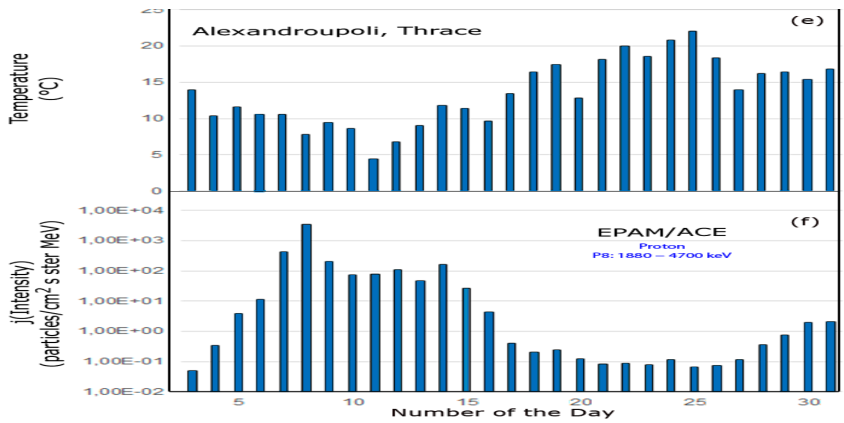

Figure 3. The data in the figure show three time intervals with rainfall in Alexandroupoli (blue bars in (**b**)) coincided with peaks in high energy solar proton P8 flux, around days 8, 14, and 30 March 2012 (**c**). During the period 6–16 March, when the energetic particles at ACE increased and then decreased, a storm series comprised of four individual storms on 7, 9, 11 and 15 March (**d**). The horizontal blue bars indicate four characteristic periods with increased high energy proton flux at ACE. The two regular blue lines indicate times when the EPHIN instrument on the SOHO satellite observed solar cosmic rays (>500 MeV protons). After these very high-energy proton events, Alexandroupoli experienced rainfall and temperature (**a**). The daily values of temperature and the ACE P8 solar high energy proton flux are strongly and significantly anticorrelated (**e**,**f**).

In panel d of Figure 3 we distinguish four magnetic storms, on days 7, 9, 12 and 15 March, with low to very extreme low values of the geomagnetic index Dst [83]. Tsurutani et al. [84,85] noted that storms S1, S2, S3 and S4 on 7, 9, 12, and 15 March (Figure 3d) appeared after ICME-associated MHD traveling interplanetary shocks on days 7, 8, 11–12 and 15.

The influence of space weather on the Earth and its environment is most often considered in terms of geomagnetic activity (magnetic storms). However, solar or galactic cosmic rays are known to influence atmospheric dynamics [3,11,31–39,42–45]. In panel c we see some flux peaks superimposed on a large time-scale flux structure starting on 4 March and ending on 20 March. We name the onset phase of the whole proton flux structure, on days 4–6, SEP-1. The solar energetic proton (SEP) events seen as particular flux enhancements on days 7–9, 11–12 and 14–15 March 2012, are called SEP-2, SEP-3, and SEP-4, respectively, and are marked by solid blue bars in Figure 3d. Both the magnetic storms S1, S2, S3 and S4 and the solar proton events SEP1–2, SEP3, and SEP4 are causally related to the appearance of AR11429 on the solar disk and the subsequent IP space disturbance, in particular, due to the CMEs accompanied solar flares F1 and F2.

The short-lived low-energy P2′ proton peaks seen after 17 March are of magnetospheric origin; they are produced by particle acceleration within the magnetosphere and escape into the interplanetary space. These low energy flux peaks show a high peak-to-background flux ratio (j_p/j_b), with $j_p/j_b > 10^2$, which is unusual for upstream protons at the position of ACE [4,85]. These high j_p/j_b values recorded far upstream from the Earth's bow shock strongly suggest that the magnetosphere was a powerful accelerator at those times.

The largest solar proton and electron flux enhancement in Figure 3, SEP-2, is characterized by a sharp peak on March 8 around the time of the ICME-related shock (panel c). In [4] we noted that the March 8 SEP event falls into a rare class of solar cosmic ray events. For instance, the P8 (1.88–4.70 MeV) protons show an unusual flux increase, with a maximum peak intensity $j > 10^4$ p (cm^2. sec. sr. MeV)$^{-1}$ and an extreme value $j_p/j_b > 10^6$ compared to the background P8 flux on March 4 ($j_p/j_b > 10^3$ compared to the pre-flare values of March 6). Furthermore, we also mentioned that the SEP-2 P8 flux ratio j_p/j_b was the highest among the CME-related SEP events observed during a period of 18 years (1997–2015) [4].

Like the energetic ions, the solar energetic electrons follow open IMF lines and precipitate in the high latitude magnetosphere, ionosphere and atmosphere, into the cusp, a region adjacent to the outer radiation belt (RB). The outer RB is a region rich in energetic electrons, which reaches higher densities during SEP events. Figure 4 shows the flux-time profiles of energetic electrons observed by the MEP90° detector of the NOAA-18 satellite during three periods, when NOAA-18 crossed the electron radiation belts and the cusp in the north magnetosphere throughout the whole SEP event lasting between 5–17 March 2012: on 8 (panel a), 11 (panel b) and 13 (panel c) March. The two lines on the top of each panel indicate differential intensities (#el/(cm^2. sec. sr. keV) in the energy range 30–100 keV (multiplied by a factor of 10) and 100–300 keV. The line at the bottom of panels a, b and c indicates the integral intensity (#el/(cm^2. sec. sr) of semi-relativistic (>300 keV) electrons

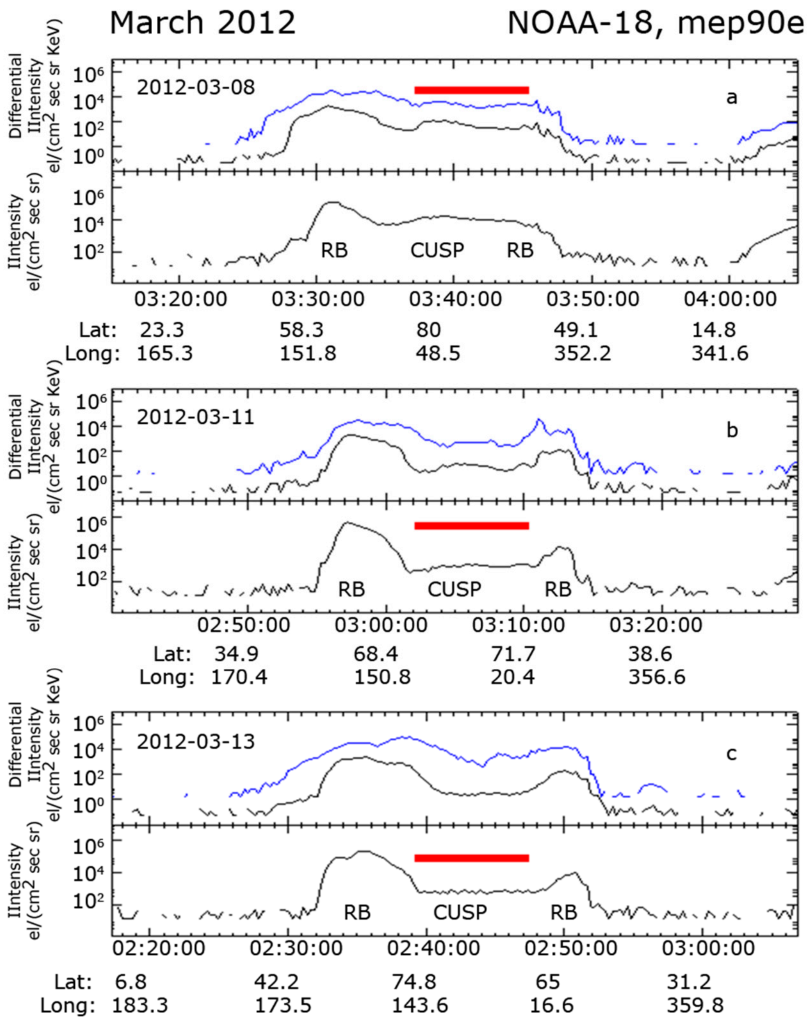

Figure 4. Flux-time profiles of energetic electrons observed by the MEP90°e detector of the NOAA-18 satellite during three periods on 8 March (**a**), 11 (**b**) and 13 (**c**). The two lines on the top of each panel indicate differential intensities in the energy range 30–100 keV (multiplied by a factor of 10) and 100–300 keV. The line at the bottom of (**a**–**c**) indicates the integral intensity of semi-relativistic (>300 keV) electrons. (**a**) depicts a rare event, with a cusp fulfilled with energetic electrons in such a way (high electron intensities) that the cusp cannot be separated from the outer radiation belts. The outer radiation belts can be well distinguished in (**b**,**c**) as two distinct structures at the edges of the whole high latitude flux enhancements. The flux drop in the cusp between ~02:40–02:48 UT on March 13 shows a >300 keV electron flux difference as high as more than 2 orders of magnitudes, between the outer radiation belts and the cusp, although the energetic electron background in the cusp was relatively high at those times (Figure 3c).

The SEP-2 event was powerful. By comparing the flux-time profiles of energetic electrons in panels a, b and c we see a plateau on 8 March at high latitudes for as long as the IP shock-related energetic electron population was reaching the Earth's environment (Figure 3c), while the electron intensity shows an increasing drop in the middle of the whole structure in panels b and c while as the solar flux was decreasing between 8–17 March (Figure 3). Panel a manifests a rare event, with a cusp fulfilled with electrons in such a way (high electron intensities) that it cannot be separated from the outer radiation.

SEP events related to SF1 and SF2 were observed by a series of spacecraft located at various sites of the heliosphere and observed protons to much higher energies than ACE. The SF1/SF2-related proton events observed within the magnetosphere by the GOES satellite showed a relative ~30 MeV proton flux enhancement >3.5 orders of magnitude [4] (Figure 1a). The solar cosmic rays observed by PAMELA from 7–9 March showed flux increases by a factor of ~10^3 at ~500 MeV [86], which suggests that the spectrum extends to energies much higher than 500 MeV. Protons with energies E > 500 MeV were also measured by the EPHIN instrument on the SOHO satellite [87]. The March 2012 solar activity was recorded on Earth as a strong decrease in cosmic-ray fluxes on the ground after 8 March [88].

In Figure 3 we have drawn two regular blue lines at the times when the EPHIN instrument on the SOHO satellite observed solar cosmic rays (>500 MeV protons). Kühl et al. have mentioned that the SOHO/EPHIN recorded these solar cosmic rays were at 4:00 UT on 7 March 2012 (SCR-1) and at 17:45 UT on 13 March 2012 (SCR-1) [86] (Table 1). As we can see from Figure 3c, the very high energy proton streams observed by SOHO coincide with the onset of SEP-1 and SEP-3 events observed by ACE.

The impact of the March 2012 solar activity was so strong so that CMEs-related shock(s) drifted much of the solar system to heliocentric distances of ~124 AU Gurnett et al. [89]. The March 7-related CMEs were also detected in Mercury's orbit by Messenger, and they caused the most intense energetic particle flows during the cruise of the Mars Science Laboratory to Mars [90].

The energetic proton flux increase and a magnetic storm on 28–30 March seen in Figure 3c indicate remnants of particle reservoir still present in the next solar rotation originating from the SEP stream starting on 4 March.

3.2. Extreme Meteorological Events in Thrace, Northeast Greece, in March 2012

In [4] we provided significant evidence that the SF1 and SF2 and the subsequent release of highly geoeffective ICMEs were responsible for the March 2012 heat wave in northeast USA. It is well known that the March 2012 heat wave was not a local extreme weather event. With the heat wave in the northeast USA, western and central Europe experienced one of the warmest Marches. Temperatures in the U.K. recorded averages 4.5 °F (2.5 °C) above normal, i.e., the warmest March since 1957, while Austria and Germany had their third warmest March on record.

On the contrary, large parts of the northwestern United States, western Canada, Alaska, eastern Asia, and Australia experienced below-average temperatures. March 2012 was also abnormally cool in southeast Europe. Heavy rains, snowfalls, and strong winds were observed during unusual winter-like spring weather in Greece. BBC NEWS website, for instance, describes the unusual March weather in Greece: « Snowstorms have caused transport chaos around the Greek capital Athens, with one overnight traffic jam stretching for up to 15 km (9 miles). Ferry services were disrupted and there were power cuts in some parts of the capital and on the islands, prompting some schools to close. . . Some roads in the Peloponnese, central Greece and the north of the country were also shut, according to the Greek news website Ekathimerini» (https://www.bbc.com/news/world-europe-12674491; accessed on 30 September 2023).

Since we found good observational evidence that the March 2012 heatwave in the northeast USA was triggered by unusual space weather following the SF1 and SF2 [4], we also know that weather anomalies were a global planetary phenomenon at that period [91]. We wanted to check whether ground meteorological extremes in southeast Europe and Greece, were well related in time with specific space weather events, as in the case of

March 2012 [4]. This second case study was selected based on the location of the university where most of the co-authors of this paper work, the Demokritos University of Thrace (DUTH), are located. DUTH extends over the geographical region of Thrace, in northeast Greece (Figure 4). Meteorological data in our study were obtained in two towns, in east and west Thrace, Alexandroupoli and Xanthi, respectively. A possible good relation of space weather with atmospheric extreme events at a specific second place on the globe (DUTH and its close region) in March 2012, besides the case of the March 2012 heat wave we previously examined [4], would greatly support space weather as the most likely candidate driver mechanism of the weather anomalies at the two sites on the globe (northeast USA—southeast Europe). Figure 5 displays a map of Greece. Alexandroupoli and Xanthi (indicated by solid red circles) are located at N40.85°, E25.87° and N41.13°, E24.89°, correspondingly in northeast Greece (southward of Bulgaria and west of Turkey.

Figure 5. Map of Greece. Ground measurements of weather parameters were measured in Xanthi, west Thrace, and Alexandroupoli., east Thrace. The two towns are marked on the map, in northeast Greece.

Firstly, we can see some characteristic features concerning a relationship between space weather at ACE, in the interplanetary space relatively near the Earth, and meteorological parameters in Alexandroupoli (east Thrace) in Figure 3. Rainfall in Alexandroupoli was recorded during three time intervals in March 2012: around days 8, 14, and 30 March 2012 (blue bars in panel b). A careful comparison of the data in Panels b and c suggests that rainfall in Alexandroupoli occurred during three major solar energetic particles (P8) flux enhancements that is around day 8–9 (SEP-2), 15–16 (SEP-4) and 30 March and that the two first periods with rainfall started after the solar cosmic ray events SCR-1 and SCR-2, which observed by SOHO at the beginning of SEP-1 and SEP-3 events. Secondly, from the comparison of the data in Figure 3 we infer that during the period 6–16 March, when the energetic particle flux increased and then decreased, a storm series occurred (panel d), after the incident of CME-related MHD shock waves/SEP events starting on 7 March.

Furthermore, during this period (6–16 March) the temperature T_A in Alexandroupoli decreased and then increased following the opposite pattern of the solar particles. In particular, the temperature decreased until 11 March from 15 °C to 3 °C, a T_A variation

$\Delta T_A = -12°$, between 3–11 March. Then the temperature increased from 3° to 23°, an increase $\Delta T_A = 20°$, until the end of the SEP event and beyond. Moreover, from the separated pair of panels e and f of Figure 3, between 3–31 March, we see an anticorrelation between daily-averaged values of T_A and P8 (the temperature in Alexandoupoli and the ACE/EPAM P8/1.88–4.70 MeV proton flux), suggesting weather cooling (warming) when solar high energy flux was increasing (decreasing). An estimation of the cross-correlation between T_A and P8 for lags $k = -3, \ldots 0, \ldots, 3$ suggests a substantial and significant ($p = 0.05$) anti-correlation with the highest correlation coefficient ($r = -0.75$) at $k = 0$. The results suggest no remarkable delay between T_A and P8 in daily data (Appendix A; Figure A1). We infer that the meteorological and space weather data in Figure 3 are consistent with space weather as a driver of the winter-like weather in Alexandroupoli between 6 and 16 March. This conclusion is further checked with more space and Earth-based measurement data in the following.

In Figure 6, we present Cloud top temperature (CTT) as made by the MODIS (Moderate Resolution Imaging Spectroradiometer) instrument onboard the Terra (Figure 6a) and Aqua satellites (Figure 6b). The CTT 1-day mean measurements of Figure 6a,b were obtained by the Terra and Aqua satellites in the region enclosed in rectangle of Figure 6c (18.3181°E, 33.2746°N, 26.5359°E, 42.1076°N). The CTT values are shown in colors corresponding to those of the color bar on the right side of Figure 6b, ranging from 1 to 30 March 2012 (horizontal axis).

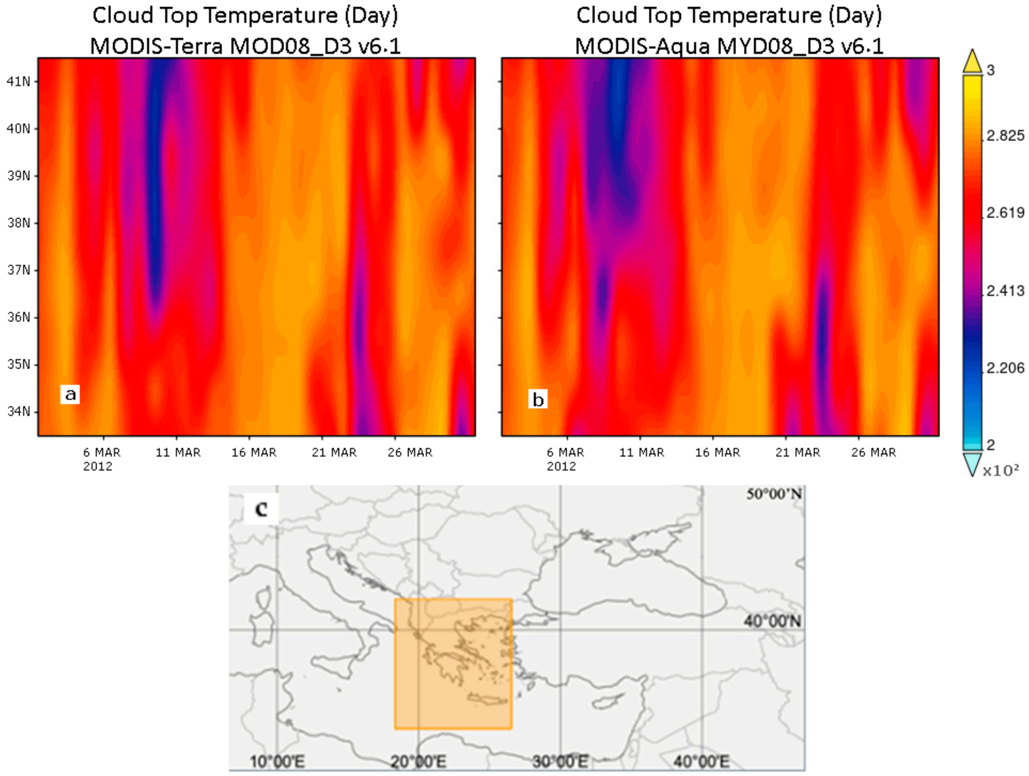

Figure 6. Cloud top temperature (CTT) as measured by MODIS (or Moderate Resolution Imaging Spectroradiometer) aboard the TERRA (**a**) and AQUA (**b**) satellites from the period 1–31 March 2012 in a region with latitudes between N33.5°–N41.5°. The lowest values were recorded by AQUA above north Greece between ~8–11 March during the major SEP-2 event of Figure 3c. The CTT color bar is in K (Kelvin). Analyses and visualizations using the MODIS Cloud top temperature (CTT) were produced with the Giovanni online data system, developed, and maintained by the NASA GES DISC. The yellow box inside (**c**) indicates the region covered by the MODIS measurements, which are shown in panels (**a**,**b**).

From Figure 6a,b, the Hovmoller-Longitudinal Average projections represent essential spatial and temporal CTT features. Alexandroupoli is located at 40.85°N. The most striking feature is the bluish-colored structure at north latitudes centered at ~400 and extending ~50 southward. A careful look at the colors of the blue structure suggests that TERRA/MODIS and AQUA/MODIS reached very low values between 9–11 (Figure 6a) and ~8–11 (Figure 6b) in March 2012, correspondingly. A comparison of the CTT values of Figure 6a,b with Figure 3c suggests that the lowest cloud-top temperature above Greece was recorded after SEP-2 occurred on 7–8 March 2012, when ACE observed the highest flux of protons in March 2012. Figure 6a shows a stable anomaly in decreasing the CTT around 9–11 March with a distinct level in comparison to the average level of CTT for the entire month of March 2012. The PM map for MODIS CTT (Figure 6b) shows a diffusion in the CTT level over the same spatial segment. This could be an effect of the afternoon migration of some humidity via the jet stream flowing from the sea towards the land and facing the cloud formation, but maintaining anomaly patterns. After some additional checks with data a year before (March 2011), MODIS CTT maps for the same region show no similarities to the 2012 MODIS CTT (Appendix B). This suggests that the 2012 drop in CTT during March 9–11 is not affected by climatology or some usual seasonal pattern in the region. In Figure 7, we examine the progress of the wind situation for fifteen days (3 March 2012–17 March 2012). In particular, Figure 7 displays daily wind fields in south Europe and the Mediterranean Sea, including Xanthi, Greece (solid red circles), resulting from NCEP Reanalysis at mid-tropospheric heights (500 hPa).

Figure 7 shows that the speed wind intensifies during two phases (8–10 March 2012 and 12–13 March 2012) throughout the continuous course of an eastward moving cyclone appearing on March 6th in the east Atlantic/west Mediterranean Sea and leaving the east Mediterranean/Middle East on 17 March; the two phases of the intensified wind speed coincide in time with the periods following the interplanetary shocks of 8 and 11 March probably suggesting a causal effect.

The wind fields indicate that strong southwesterly winds prevailed in the central Mediterranean on days 8–10, favoring the transfer of moist air from the central Mediterranean into the Greek territory. A cyclone further reinforced these winds, which initially developing Greece and then moved north into the Greek area. The combination of the moist air and the subsequent low-pressure conditions over Greece (allowing the uplift of the moist air) set favorable conditions for rainfalls in the Greek territory. These conditions coincide in time with the very low cloud top temperatures recorded by MODIS on TERRA and AQUA on March 8–11 at an extended range of latitudes (Figure 6), after the arrival of the major SEP-2 event (7–9 March 2012; Figure 3c). In Figure 8, we present CTT measurements made by the MODIS instrument onboard the TERRA satellite, but at the Xanthi longitude. CTT is indicated as a function of latitude and time, ranging from N30° to N70° (horizontal axis) and from 4 to 13 March 2012 (perpendicular axis), respectively. The temperature (T) values are shown in colors corresponding to those of the color bar seen below the figure. From Figure 8, we can see some important spatial and temporal features. The most striking feature is the blue-colored structures on days 8–10 March 2012.

A comparison of the T values of Figure 8 with SEP fluxes in Figure 3c suggests that the lowest cloud-top temperature above Alexandroupoli started recording by MODIS/TERRA after ~1 day from the onset of the SEP-2 event, that is about one day after the arrival of the March major SEP-2 event (7–8 March 2012) ACE observed, although low CTT is seen on March 7 as well.

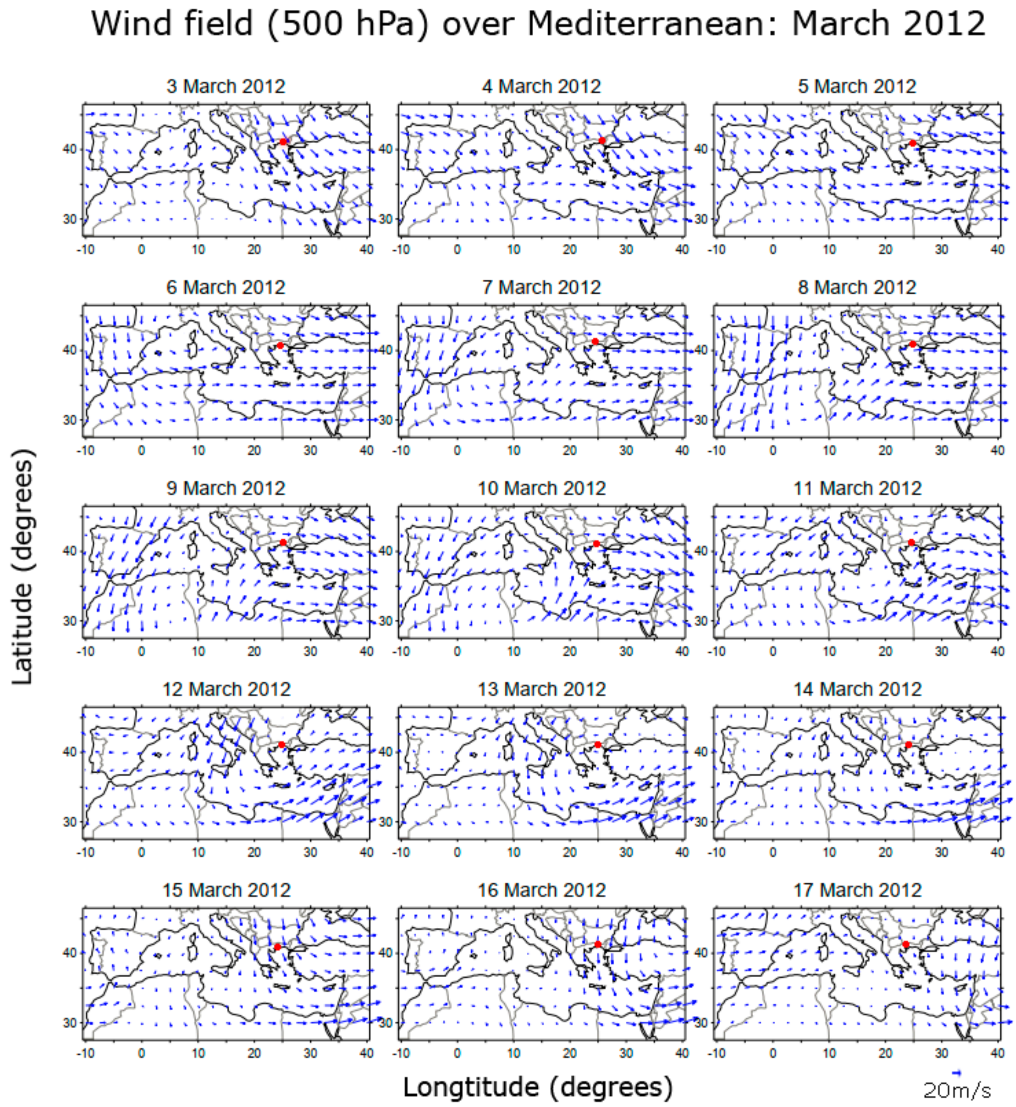

Figure 7. NCEP Reanalysis-provided daily wind fields at mid-tropospheric heights (500 hPa) for 3–17 March 2012. The location of Xanthi, Greece, is shown by a solid red circle. The blue arrows in the figure of each day indicate the wind velocity compared to the arrow corresponding to 20 m/s right bottom corner. Thrace (solid red circle) experienced particularly intense cyclonic circulation, during two periods of ICME-related magnetic storms on 8–10 (northward streaming) and 12–13 March (southward streaming).

Furthermore, it is worth noting that the TTC drop structure was recorded by MODIS at a region of longitudes centered at ~40° and extending ~5° northward and ~5° southward. A careful look at the colors of the blue-green structure seen between 4–15 March 2012 suggests that the temperature T ranged between ~0 °C–~63 °C (~210 °K–~273 °K). Therefore, we infer that between 4 and 13 March 2012, the top of the cloud above Alexandroupoli, was colder, suggesting appropriate conditions for precipitation [92]. A second T drop (green colors) in Figure 8, around Alexandroupoli's latitudes was recorded between the middle of days 14 and 15 March. This temperature decrease on the top of the clouds was re-recorded ~1 day after the arrival of the SEP-4 event (~13–15 March 2012), the second major particle event seen in Figure 3c.

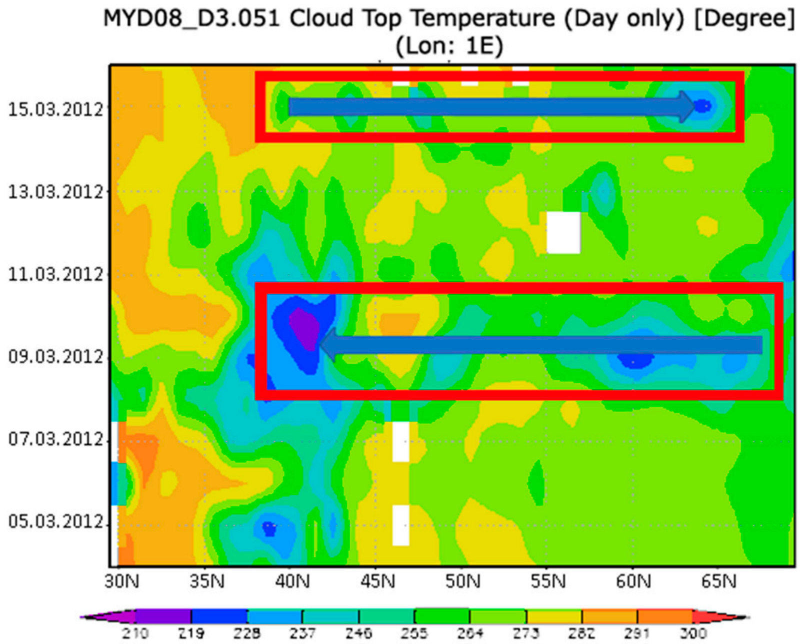

Figure 8. Top cloud temperature T as measured by MODIS (Moderate Resolution Imaging Spectroradiometer) aboard the Terra satellite, during 5–15 March 2012 in a region with latitudes between N30°–N70°. The lowest T values were recorded above north Greece, at middle latitudes (~41°N), between ~9–11 March during the major SEP-2 event of Figure 3. It is worth noting that the CTT drop structure recorded by MODIS/TERRA on 8–11 March 2012 appears to be a large structure over the middle and high latitude Europe, at Greece longitudes (~40°), extending all the way from ~35°N to >70°N, which is consistent with the large scale extreme events appearing in the globe (i.e., heatwave in northeast USA [4]). The blue arrows in the two red rectangles indicate the general opposite CCT gradient direction at periods ~9–10 and ~14–15 March 2012 (corresponding to the front and the back side of the eastward moving cyclone shown in Figure 7).

It is worth noting that the CTT drop structure recorded by MODIS/TERRA on 8–11 March 2012 (T1) appears to be a large structure over the middle and high latitude Europe, at Greece longitudes (~40°), extending from ~35°N to >70°N, which is consistent with the large scale extreme events appearing in the USA and the North Atlantic [4] and the global character of meteorological extreme events at those times [91]. It is also worth noting that the second period with CCT drop, between 13–15 March 2012 (T2) suggests a large region with CCT decrease, but this event, T2, is slighter than T1, and shows minimum CCT at high latitudes around 65°N. In Figure 6 we show (by blue arrows in red rectangles) the general opposite CCT gradient direction between T1 and T2 events.

Figure 9 displays the cloud cover all over the planet according to the MODIS/Aqua measurements on 6 March 2012 (panel a) and 10 March 2012. Panels a and b indicate the cloudy covering of Earth before (6 March) and after (10 March) the arrival of the ICME-related SEP-2 event, which bombarded the Earth's environment, in particular the cusp, with a flood of high energy ions and electrons (Figures 3 and 4). We have already discussed in [4] the large-scale atmospheric dynamics in Northeast America and the North Atlantic, characterized by an anti-cyclone in the North Atlantic providing warm air transported from the Gulf of Mexico in the northward direction. Figure 9 helps us to realize the large-scale weather variation taking place from 6 to 10 March 2012 eastward from the North Atlantic anti-cyclone, in the whole region from northern Africa to north of Europe (yellow rectangle). We see that the clear sky over almost the whole of Europe on 6 March (panel a) changed dramatically into a much cloudier sky above northern Africa, the central Mediterranean, the southeast Europe and a broad region inside the northern European coasts after the ICME-related SEP-2 event (Figure 3), on 10 March (panel b; brown colored areas). Furthermore, it is worth noting that in some European countries, like Belarus and

Norway, the rainfall started on 10 March, while some regions experienced precipitation earlier, such as in Hamburg, Germany (on 7 March).

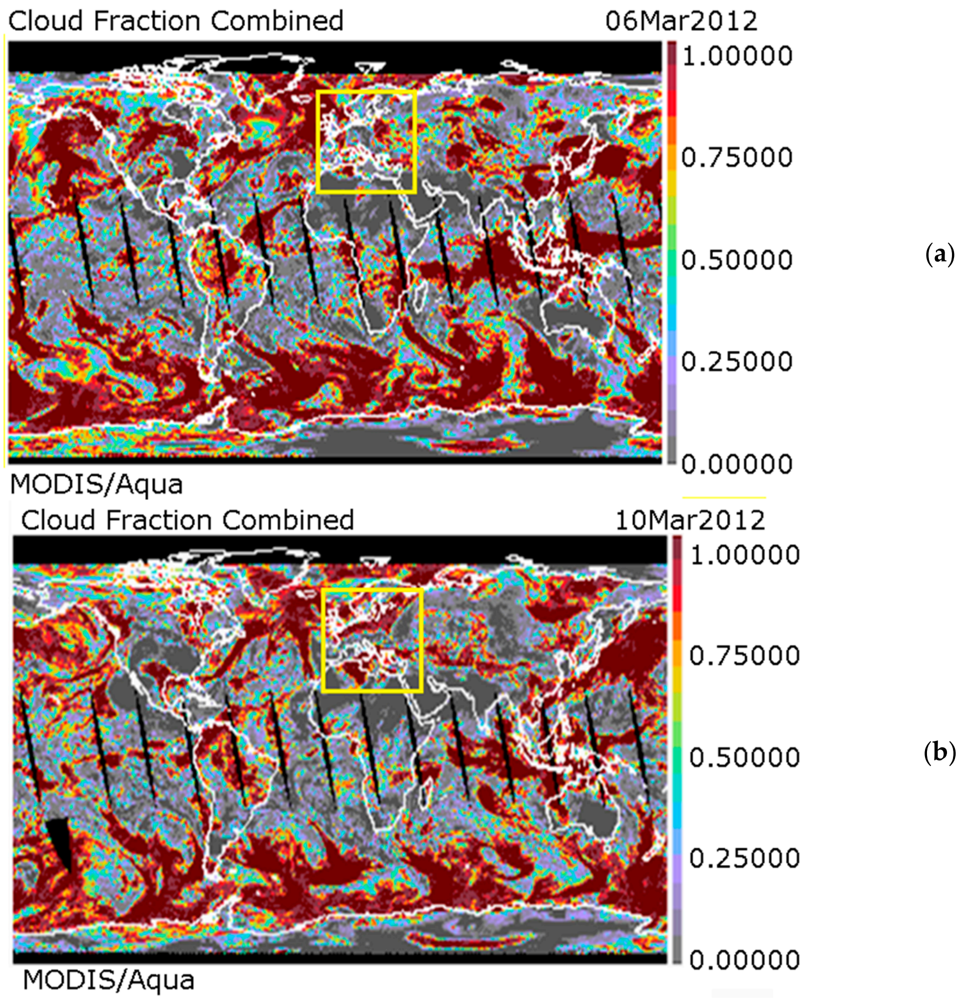

Figure 9. Cloudy all over the Earth according to the MODIS/Aqua measurements on 6 March 2012 (**a**) and 10 March 2012 (**b**); the yellow rectangle in (**a**,**b**) indicate the region of interest in this study. The clear sky over almost the whole of Europe on 6 March (**a**) changed dramatically into a much cloudier sky above North Africa, the central Mediterranean, southeast Europe, and a broad region inside the northern European coasts on 10 March ((**b**) brown colored areas), after the detection of the ICME-related SEP-2 event by ACE (Figure 3).

The cloud cover shown in Figure 9 is consistent with the cloud top temperature seen in Figure 8. It suggests the existence of a large-scale atmospheric anomaly that affected northern Africa, the Mediterranean and the Aegean Sea, southeastern and northern Europe on 10 March. Furthermore, the cloudy **conditions** in the Mediterranean, the Aegean Sea, northern Africa and the southeastern Europe –including Greece- are consistent with the enhanced wind speeds of the anticyclone extending over these regions, as we saw in Figure 7. We recall that these weather disturbances occurred after the detection of the shock-related SEP event by ACE on 7–8 March and during the subsequent large magnetic storm onset on 9 March.

Figure 10 displays detailed meteorological measurements (courtesy of Pr. Kourtidis and Dr. Kastelis) from a station on the Campus of our Democritus University of Thrace (41.15°N, 24.92°E, 75 m above sea level), in the town of Xanthi, ~90 km westward of Alexandroupoli (40.8°N, 25.8°E, Greece). The station is located approximately 3 km from the city center of Xanthi; thus, it is characterized as rural, and the city does not influence it.

In particular, the measurements in Figure 10 shows in detail the values of the atmospheric Potential Gradient (PG; Refs. [93–95] of the electric field (red line), the wind speed (black line), and the accumulated precipitation (purple shaded region) during the period 5–15 March 2012. Figure 8 displays values of the electric field, wind speed, and accumulated precipitation, which suggests extremely bad weather starting on March 8 and continuing until the end of the time interval examined (15 March 2012).

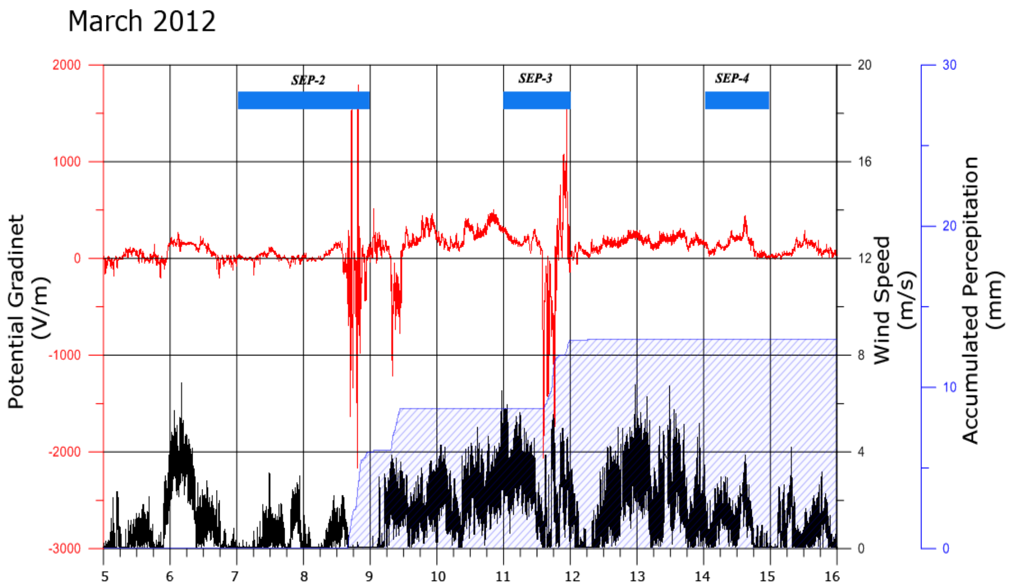

Figure 10. Atmospheric Potential Gradient (PG) of the electric field (red line), the wind speed (black line), and the accumulated precipitation (purple shaded region) between 5–15 March 2012. In the second half of the days 8 and 11 March, large fluctuations of the atmospheric electric field were recorded after the incident of two interplanetary shocks on Earth. Winds and rainfall accompanied the AEF fluctuations.

From Figure 10 we see that the meteorological station in Demokritos University of Thrace recorded three large-amplitude electric field fluctuations after the two IP shocks detected by ACE at ~11:30 UT, on 8 March and at ~12:28 UT on 11 March, and the maximum SYM-H at 07:58 UT on 9 March as reported by [84]. Important to note is that the unusually large-amplitude electric field fluctuations in the second half of 8 March, ranging between ~−2000 V/m–~1800 V/m, appear after the strong 8 March IP shock. It is also worth noting that both shock-related EFFs (~11:30 LT on 8 March and ~12:28 LT on 11 March) show a fluctuation profile reaching large positive and negative values. On the contrary, the S2 magnetic storm-related AEF only displays negative electric field excursions at low values (~1000 V/m). In Figure 10, the periods of SEP-2, SEP-3 and SEP-4 related with IP space structures incident on the magnetosphere are also marked with a blue bar for comparison.

Figure 10 clearly shows that the 8, 9 and 11 March EFFs were followed by rainfall and winds (purple and black lines). It is worth noting that the increases in the accumulated precipitation were more significant after the shock-associated bipolar EFFs than after the storm-associated negative electric field anomaly.

The space and terrestrial data shown above suggest that the extreme meteorological events occurring in March 2012, particularly between 8–11 March were related to unusually intense solar activity and unique weather events, as in the case of the March 2012 heatwave in the northeast USA.

3.3. Perturbations in the High Voltage Electric Power Grid in Thrace, Greece, in March 2012

Since we have found good evidence of correlations between unusual meteorological variations in Thrace (Xanthi, Alexandroupoli), Greece, and the ICME-related SEP events in March 2012 that followed the occurrence of SF1 and SF2, in this section we examine the possible influence of space weather on the electric grid in the same region and at the same time period.

For this reason we investigate the possible relations of the March 2012 space weather events with possible perturbation in the high (150 kV) voltage electric power network in Thrace, north-east Greece, as recorded by the SCADA system of the Independent Power Transmission Operator (IPTO), in Komotini. Komotini is a town located between Xanthi and Alexandroupoli and is the capital of the local geographical region of Thrace. This second study of the present paper concerns the time period of 5–15 March 2012, which includes the major space weather events observed after SF1 and SF2 (Figures 2 and 3).

Since a series of papers have shown that during the incidents of intense ICMEs on Earth's magnetosphere geomagnetically induced currents (GICs) are often recorded on ground level, which cause inconveniences to the electric power systems, we wanted to examine whether the electric IPTO grid in Thrace was affected by the geoeffective storm series of March 2012, and, furthermore, if the cause of the possible electric current perturbations might be separated from the unusual meteorological events taking place in the same time period.

The IPTO factory's SCADA system records the voltages between the phases L1-L2, L2-L3 and L3-L1 in the connection point of the voltage output from the factory with the high voltage electric power grid every 1 s. In the present study we analyze 1 s and 1-h averages of such data. So, in Figure 11 we show 1-h averaged data for selected days during the time period 5–15 March 2012. The data shown were created by processing the time-average values of the three 1 s voltages between the phases L1-L2, L2-L3 and L3-L1. From the 3600 values per hour, the maximum MAX (blue lines) and the minimum MIN (green lines) values per hour were determined. Furthermore, from the MIN and MAX values, we created a time series of the differences (DFR = MAX − MIN) between the 1-h averaged maximum and minimum voltage values. The presented DFR values show the result of the actual DFR values added to the level of the 153 kV standard voltage value (red lines) to avoid confusion with the other (MAX, MIN) lines.

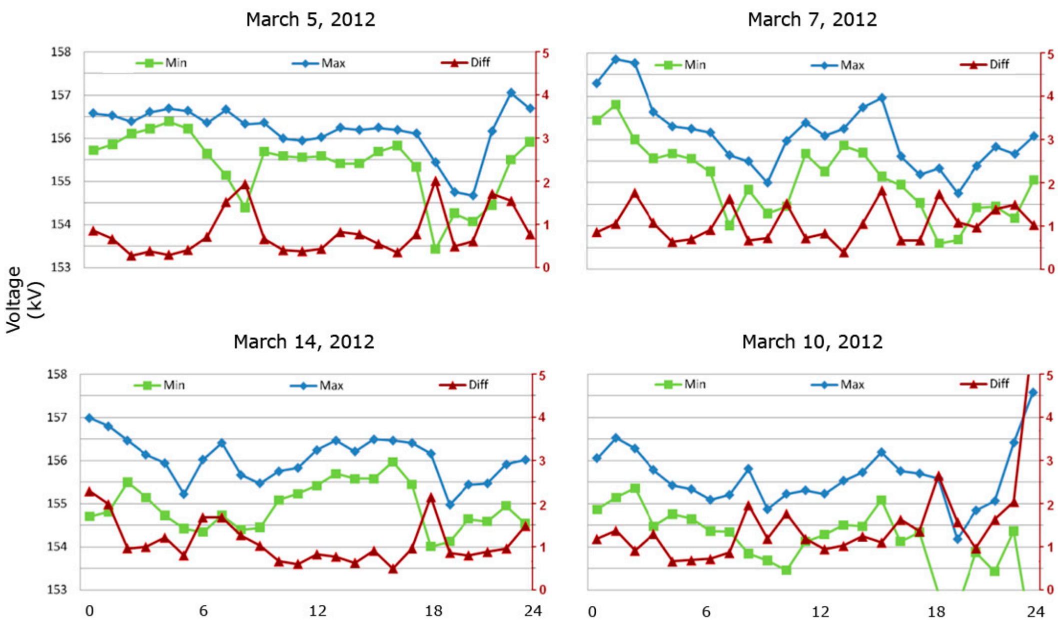

Figure 11. Daily diagrams during the period of 5–15 March 2012 for the minimums (MIN; green curves) and the maximums (MAX; blue curves) of hourly averaged values of the three voltages (L1, L2, L3) for the 150 kV transmission network in Thrace, Greece, as well as their difference DFR (red curves), for each hour of the day. The graphs on 5 and 14 March represent magnetically quiet days, with two peaks in the morning and the afternoon. The graphs on 7 March and 10 March represent disturbed days displaying several peaks of comparable values.

Panels a and b on the left sides of Figure 11 present the 1-h MAX, MIN and DFR voltage values on days 5 and 14 March, which were recorded under quiet magnetic conditions (Figure 3), well before and after the major SEP-2 event observed on days 7–9 March 2012 (Figure 3c).

The elaboration of the graphs in panels a and b reveals the appearance of a daily cycle of voltage changes in the 150 kV transmission network at periods around 7:00 LT–9:00 LT and 18:00 LT–20:00 LT. The MIN voltages in the early morning hours (7:00 LT–9:00 LT) correspond to times when inhabitants of Northern Greece are preparing to go to their place of work, while the MIN values in the afternoon hours (18:00 LT and 20:00 LT) correspond to times when the workers return homes, coinciding with the night darkness start; in the morning hours (7:00 LT–9:00 LT), the night-lights turn off and the companies' activity start, and in the evening hours (18:00–20:00), the night-lights turn on due to household and public lighting activation. The peaks in DFR voltage (red line) at the 150 kV transmission network in the morning and the afternoon, were unveiled on both days 5 and 14 March, and they were present in all daily graphs checked for the interval 4–15 March 2012.

Panels c and d, on the right side of Figure 11, show the 1-h averaged MAX, MIN and DFR voltage values obtained by IPTO during days 7 and 10 March 2012, and they are presented in the same format as in panels a and b. During these days, 7 and 10 March 2012, the Dst index reached low values (Figure 3d), suggesting that magnetic storms were in progress, due to the arrival of SEP-2 and the associated ICME, respectively. It is evident that the MAX, MIN and DFR voltage profiles during the two storms (panels c and d) are different from those during the magnetically quiet days (panels a and b).

In particular, we see that the two significant DFR peaks in the morning and afternoon of the quiet days were divided into several voltage peaks of comparable values during the magnetically disturbed days of 7 and 10 March 2012. It is also remarkable that the general DFR background increases in prenoon-noon-afternoon times (11 LT–18 LT) on 10 March, during the recovery phase of the major magnetic storm of March 2012.

In Figure 12, we present high-time resolution voltage data of 1 sec from IPTO for the period 5–15 March 2012. These data have been processed and presented to examine steep and sudden changes in the high voltage values, and we defined "steep" or "sudden" change in the high voltage, as a voltage change greater or less than 500 V compared to the existing average voltage value in the last 5 s (Appendix C). These changes were determined for each day, during the period 5–15 March 2012, and are plotted in the graphs of Figure 12 as overvoltage (positive values) or voltage drop (negative values) points.

From a comparison of the data of Figure 12 with those of Figure 10, we infer that the diagrams of sudden voltage changes (SVC) within 1 sec follow, in general, the standard pattern of the 1-h averaged voltage data, with almost permanent events in the morning, between 07:00 LT–09:00 LT and in the evening, between 18:00 LT to 20:00 LT, but also at post-noon times (14:00 LT–15:00 LT), when the citizens have their lunch. We note that the duration of each event, which starts with a sudden voltage increase, is reflected by the number of "anomalous" points (SVC > 500 V) than the current average voltage value in the last 5 s.

The most characteristic feature revealed from Figure 12 is that SVCs appear many more times ("anomalous" points) on magnetically disturbed days (7 and 10 March 2012; Figure 10) than on the quiet days (5 and 14 March 2012; Figure 11). For instance an elaboration in Figure 10 suggests that 37 SVCs were recorded on March 10, with maximum daily value of the voltage surge creation/voltage drop 3.61 kV/–3.32 kV. On the contrary, only 7 SVCs were recorded on March 5, with the maximum daily value of the voltage surges creation/voltage drop 0.89 kV/–0.66 kV. Detailed information on the daily number of SVCs, along with the maximum value of the voltage surges created and the voltage drop on each day between 5–15 March, is given in Appendix D.

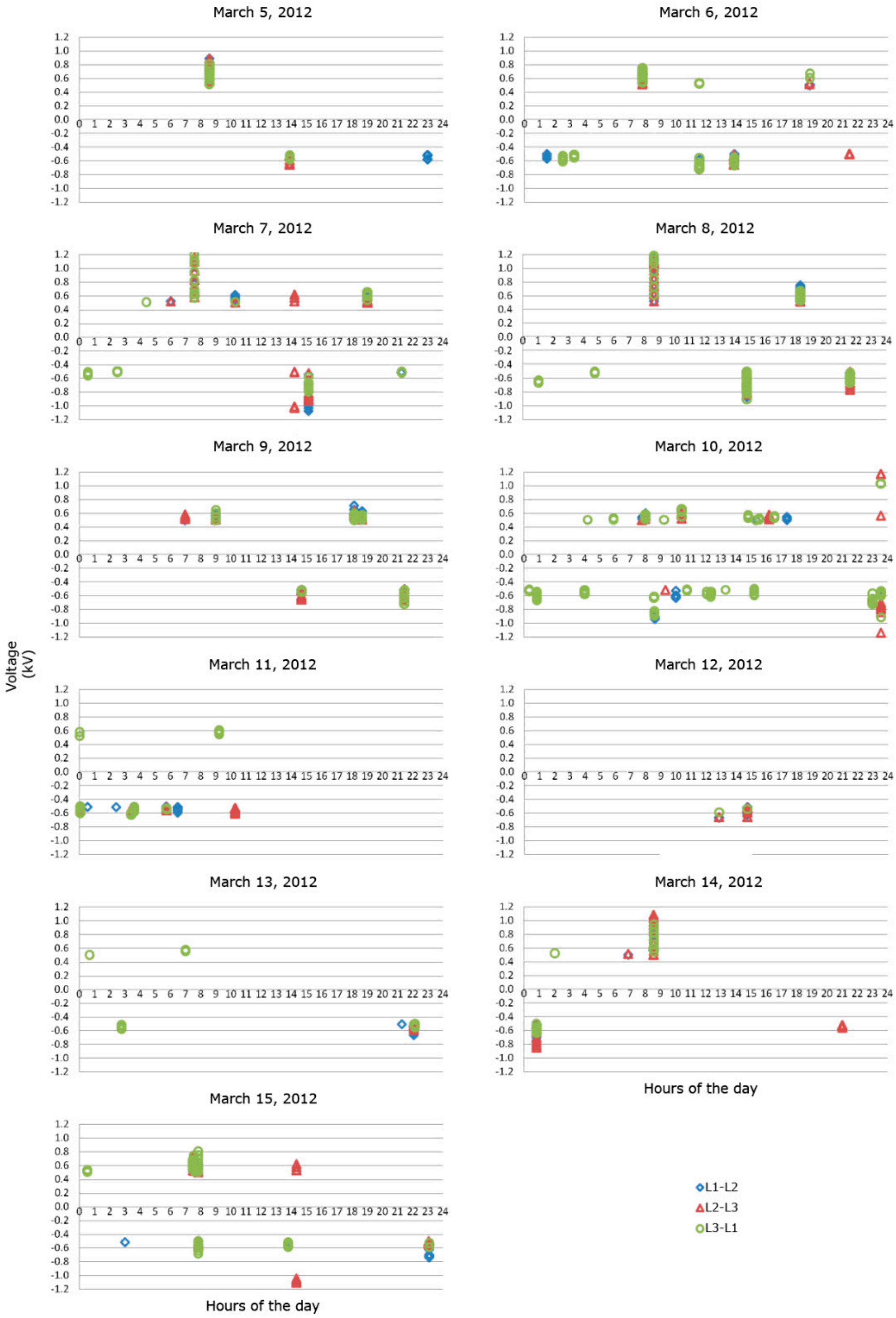

Figure 12. Daily charts (covering the period 5–15 March 2012) for steep and sudden changes for the three phases L1-L2 (blue marks), L2-L3 (red marks), and L3-L1 (green marks) on the transmission network of 150 kV in Thrace. Although, the reader can note the moments (morning, noon, and evening) when massive human activity is evident, there are points, on some days, which cannot be explained by human activities. It is worth noting that the highest number of anomalous voltage changes were recorded on 10 March, during the decay phase (slowly varying magnetic fields) of the major storm in March 2012, observed after the incident of an ICME-related interplanetary shock.

We point out that the results of Figure 12 are in agreement with the results of the hourly averaged data of Figure 11. Furthermore, a comparison between the number of SVC events on days 9 and 10 March 2012 suggests that much more sudden disturbances occurred in the electric grid in Thrace on 10 March than on 9 March. This is probably a significant result, since the magnetic storm on 10 March showed slow geomagnetic field B variations, during the recovery phase of the storm, in contrast to 9 March, when the storm was characterized by abrupt B field changes, during the storm main phase (Figures 3 and 13). In addition, the highest value (3.61 kV) of the sudden voltage drop and the surges creation was recorded on 10 March 2012. This result needs further investigation in the future, to examine whether such an increased number of SVC events in electric grids at middle latitudes is a preferential feature of the recovery decay phase of large storms. We should note that the continuation of the high occurrence frequency of SVC events until the end of the recovery phase of the storm, that is within the first half of day 11 (Figure 12), may be an indication of a relation of SVI events on the IPTO electric grid in Thrace with slowly changing geomagnetic fields (Figure 13), which produce quasi-DC electric currents on the ground. In Figure 13, the periods of SEP-2, SEP-3 and SEP-4 and the magnetic storms S1, S2 and S3, related with IP space structures incident on the magnetosphere are marked (blue bars). The storms are the cause of the SVCs, while the SEP events with weather changes.

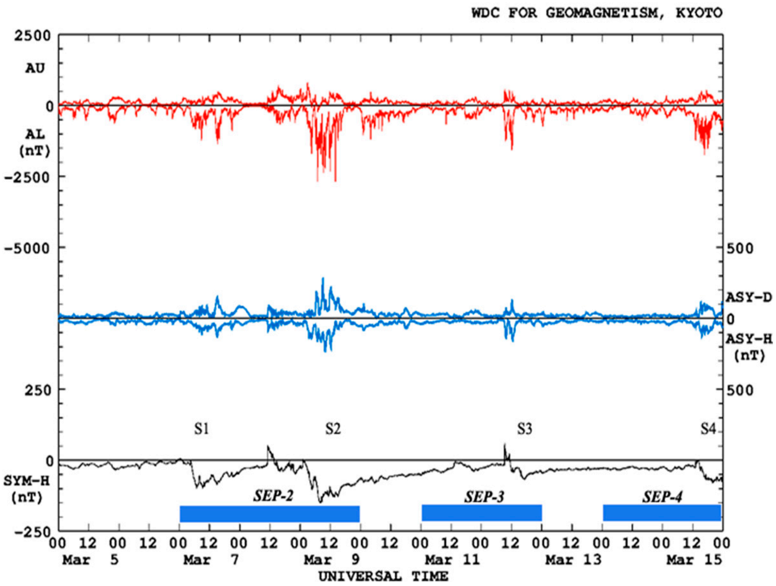

Figure 13. Geomagnetic indexes (AU, Al, ASY-D, ASY-H, SYM-H) during 5–15 March 2012. A series of magnetic storms were seen around 7, 9, 12, and 15 March 2012. The stronger storm lasting from March 7 to March 11 related to the major ICME/SEP event observed by ACE in March 2012 (Figure 3c,d). The most anomalous voltage events were recorded in March 2012 (Figures 11 and 12) during the decay phase of the major storm in the period examined.

During the period examined in Figure 12 (5–15 March 2012), IPTO recorded 203 SVC events under the criterion we used to select the voltage variations in the network in Thrace. We assumed anthropogenic agents caused all SVC events between 7–9 and 21–23 LT, and we found that 67 of the 203 events were observed in the two special periods, in the morning and the early night. Then, it is implied that a number as high as 136 events might be storm-related (Appendix D). This result reveals that IPTO recorded a significant number of SVCs during the whole SEP event and the associated series of storms in early March 2012 (within only 11 days). On the other hand, the great total (storm-related) number of 37 (28 SVC) events recorded throughout the day 10 March 2012 (Appendix D) suggests that one ~24-h time interval was of particular interest, from the point of view of storm effects in the network in early March 2012.

Figure 14 shows lightning records in Greece between 8 March and 10 March 2012. It is evident that no lightning phenomena were recorded in Thrace, northeast Greece, during times of bad weather (intense precipitation, strong wind, great ground electric field fluctuations) and voltage perturbations in the local electric grid. In contrast, intense lightning activity is evident in the middle Mediterranean on 10 March, during strong winds (Figure 7). We infer that the sudden high voltage changes found in the power electric grid in Thrace (Figures 11 and 12), for instance on 10 March, cannot be attributed to lightning effects. They are related to the particular space weather conditions at those times. It is worth noting that the lightning activity seen on 10 March was recorded during cloudy and anticyclone-strong winds (Figure 7).

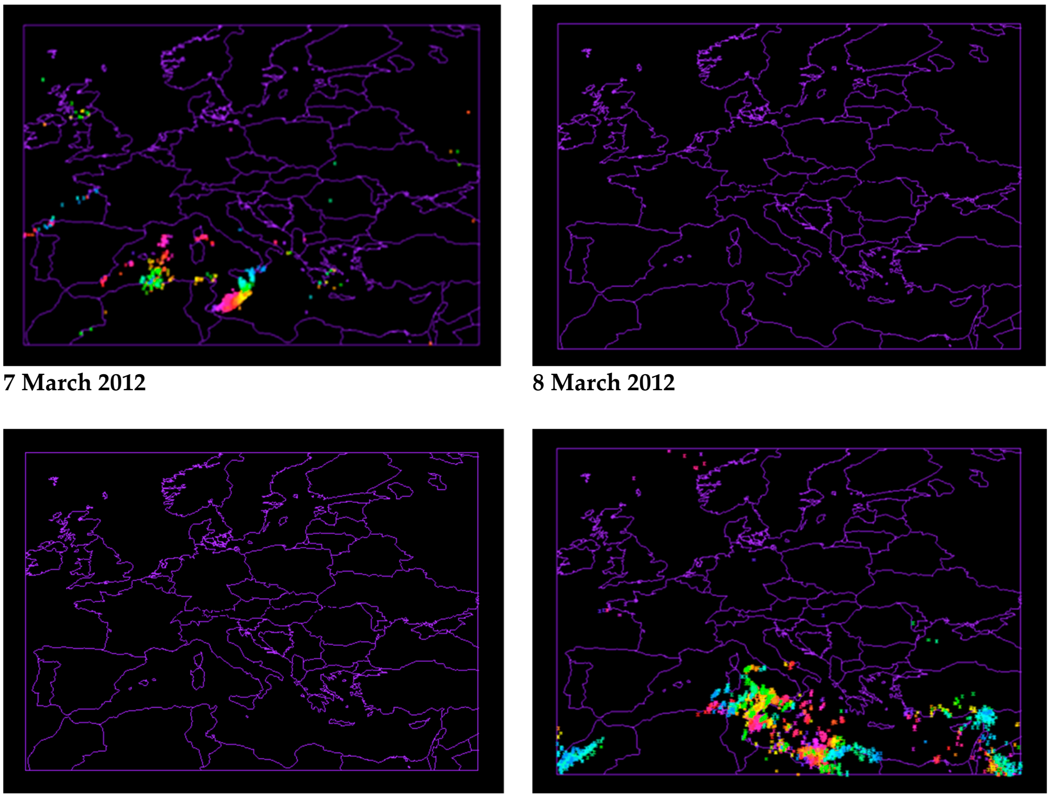

7 March 2012 **8 March 2012**

9 March 2012 **10 March 2012**

Figure 14. Lightning phenomena in Greece between 7–10 March 2012; the SVCs in the power electric grid in Thrace on 10 March (Figures 11 and 12) cannot be attributed to lightning effects.

4. Summary of Observations and Discussion

It is well known that the Sun influences Earth's Climate and weather. However, there is a need for further research on this topic, in particular, because of the global climate changes of the last two decades. In this perspective, the solar contribution on weather extremes and climate changes should be carefully estimated.

In [4] we presented a case study concerning the possible solar origin of an important extreme event. In particular, in [4], we have demonstrated that the famous March 2012 and the historic March 1910 heatwaves in the northeast USA both occurred during ICME-induced storms. We noted a common extra-terrestrial condition during both the M2012HW and M1910HW. The two heatwaves occurred during the weakest solar cycles (SC) in the last 120 years (SC4 and SC14). Since the M1910HW occurred before the GHG effect and was evidently a natural, non-anthropogenic, event, Ref. [4] inferred that we should accept that the two extreme events (March 2012 and March 1910 heatwaves) had a common origin: solar activity. Furthermore, it is worth noting that the March 2012 heatwave was characterized (i) by the arrival, near the Earth, of solar cosmic radiation with a proton spectrum extending to unusually high (>0.5 GeV) energies and (ii) a positive North Atlantic Oscillation index.

We inferred that the comparison of space and terrestrial data suggests that the hypothesis of a solar influence on the historic March 2012 heatwave cannot be rejected.

Since the March 2012 heatwave was not local in the northeast USA, but a global atmospheric anomaly [91], we wanted to further check the possible relation of the unusual solar and space weather in March 2012 with meteorological extremes far from the place where the heat wave was experienced. This second case study was selected based on the location of the Demokritos University of Thrace (where most of the co-authors of this paper work): in Thrace, Greece.

To this end we examined a lot of remote sensing instrumentation to investigate likely related physical processes in March 2012 in a variety of space regions: Sun (SDO satellite), Interplanetary Space (ACE satellite), Earth's magnetosphere (Earth-based measurements), Top Clouds (TERRA and AQUA satellites), ground atmospheric environment (Earth-based instruments).

Some of the important findings of our research concerning the possible space weather influence on the atmospheric conditions in Thrace, Greece, are the following:

(1) Unusual bad weather occurred in Thrace, Greece, which started on 6 March 2012 and lasted until ~15 March 2012: low temperatures, fast winds and intense precipitation occurred during most of this time period (Figures 3a,b and 6–10).

(2) During the above period (6–15 March 2012) of bad weather in Thrace, the ACE satellite recorded high fluxes of solar energetic ions and electrons (Figure 3c), which were related to the presence of a series of ICMEs and magnetic storms (Figures 3d and 13; see also [4,14,84]).

(3) Local measurements in Demokritos University of Thrace, in Xanthi, revealed unusually large amplitude atmospheric electric field Ez fluctuations, after the arrival of two interplanetary shock waves at ACE, on 8 March and 11 March, respectively. Both times of anomalous *Ez* were followed by storms with intense rainfall and fast winds (Figures 6 and 8).

(4) The first electric field *Ez* disturbance on 8 March was the major one, ranging between ~ -2000 V/m–~1800 V/m (Figure 10); the related storm, which lasted in Xanthi from 8 to 11 March 2012, was accompanied by a deep drop in the cloud top temperature as measured by MODIS/TERRA and MODIS/AQUA.

(5) The winter-like 8–10 March 2012 atmospheric events occurred after the detection of the SEP peak flux (8 March 2012; Figure 3c), which accompanied the main ICME that reached the Earth after two intense solar flares on 7 March 2012 (Figure 2 and [4]).

(6) During the 8–10 March 2012 atmospheric event the front of a cyclone appeared in Thrace as a northward jet stream flow, in the direction from the Mediterranean/Aegean Sea to land (Figure 7). MODIS/TERRA measurements suggest that during this period the cloud top temperature drop effect extended to a large range of latitudes, from ~35°N up to at least ~70°N, with a decreasing impact towards higher latitudes.

(7) The winter-like 12–13 March 2012 jet flow was streaming from the northward direction (higher European latitudes) and it produced the highest speeds. Still, it left no great signal of cloud top temperature drop in MODIS/TERRA and MODIS/AQUA records (Figures 6 and 8). MODIS/TERRA measurements suggest that during this period the cloud top temperature drop effect is more evident at latitudes northward of Xanthi.

(8) Daily wind fields in south Europe and Mediterranean Sea, including Xanthi, Greece (Figure 6) at mid-tropospheric heights (500 hPa) show that the speed of wind intensified during two phases (8–10 March 2012 and 12–13 March 2012) in the course of a continuously eastward moving cyclone which appeared on 6 March in east Atlantic/west Mediterranean Sea and left the east Mediterranean/Middle East on March 17th; these two phases of intensified wind speed coincides with periods following the interplanetary shocks of 8 and 11 March.

(9) During March 2012 precipitation in Alexandroupoli, east Thrace, was recorded during three periods with solar proton flux enhancements at ACE (Figure 3b,c); the two first periods with rainfall started after solar cosmic ray streaming (>5 MeV protons)

observed by SOHO. Between 3–31 March, the temperature in Alexandoupoli and the ACE/EPAM solar P8/1.88–4.70 MeV proton flux showed a strong ($r = -0.75$) and significant ($p = 0.05$) anti-corelation, suggesting weather cooling (warming) weather when the solar high energy flux increased (decreased).

(10) Sudden voltage changes (SVCs) within 1 sec (SVC > 500 V than the existing average voltage value in the last 5 s) in the high (150 kV) voltage electric power network in Thrace were recorded on magnetically disturbed days (i.e., 7 and 10 March 2012; Figures 10 and 11).

(11) Many more sudden voltage disturbances occurred in the electric grid in Thrace on 10 March than on 9 March indicating a preference for the recovery phase of the storm (Figures 12 and 13).

In the following we will refer to the above conclusions 1–12 as Points #1–11.

4.1. March 2012 Space Weather and Atmospheric Extremes in Thrace, Greece

The present second case study dealing with the possible relationship of the solar/space activity with extreme atmospheric events in March 2012 allows us to make essential conclusions on the possible cause of winter-like weather in Thrace, Greece.

Point #1 compared with the results of [4] allows the hypothesis that the unusual March 2012 heat wave in northeast USA and the bad weather in northeast Greece, which started on the same day, 6 March 2012, may have the same root cause. In addition, Points #2–6 and #8–9 suggest that the periods of March 2012 with bad weather in Thrace occurred after SEP events observed earlier in the interplanetary space by the ACE satellite (as in the case of the March 2012 heat wave in northeast USA).

In particular, Points #3–6 and Point #8 suggest that the highly geoeffective ICME-related SEP event [4], with a flux peak on 8 March 2012 was most probably the root cause of the extreme weather event that occurred on 8–10 March 2012 in Thrace, Greece, and in the east Mediterranean as well. The space origin of the 8–10 March 2012 extreme meteorological event is greatly supported by the fact that, throughout a long-lasting eastward moving cyclone (6–17 March) in the Mediterranean Sea, the wind speed became highest only during periods (8–10 and 12–13 March 2012) following the incident of two interplanetary waves/solar cosmic rayon/into the Earth's magnetosphere. The detailed meteorological measurements made in Xanthi suggest that the large electric field fluctuations, rainfall and winds on March 8 started after >1.5 days from the occurrence of the solar flare of 7 March, in agreement with the early results of Schuurmans [33].

It is worth noting that the 8–10 March 2012 extreme event in Thrace was related to a deep drop in CTT, which extended to a long range of middle and latitudes (~$-35°$->70°N at Xanthi longitude). The CTT deviation recorded by MODIS/TERRA on 8–10 March 2012 decreased with increasing latitude and it was evidently a result of northward streaming air flows from the Aegean Sea/Mediterranean (Point #6). The cyclone being in progress at those times in the whole Mediterranean, at longitudes between $-10°$W to ~28°E (Figure 6) and the CTT deviation between ~$-35°$->70°N (Point #6) reveals that the bad weather in northeast Greece examined in the present paper was a part of a large scale weather anomaly. This conclusion is in agreement with the well-known fact that the a global weather anomaly was in progress on the planet after 7 March 2012 [4,91], when solar cosmic rays started arriving at the Earth's environment due to the two large solar flares that occurred at the beginning of the same day (Point #5).

In [4], we discussed the March 2012 magnetic storm series in reference to a set of 28 large magnetic storms that occurred between August 1997 and March 2015. The set of these storms was selected by using as a selection the minimum value of the geomagnetic index Dst during the March 2012 magnetic storm series (minimum Dst = -150 nT); the set of the storms was collected under the criterion Dst ≤ -150 nT, that was a set of storms larger than the March 2012 magnetic superstorm, in a period of about 18 years. The March 2012 storm-related SEP event was characterized by the fact that the ACE satellite recorded the highest energetic (1.88–4.70 MeV) proton intensity j ($j > 10^4$ p (cm2. sec. sr. MeV)$^{-1}$)

and peak-to-background value $j_p/j_b > 10^6$; Figure 3c) among all 28 SEP events related with the largest (Dst < −150 nT) magnetic storms examined in [4].

This particular feature of the March 2012 ICME may suggest that the solar cosmic rays and not the magnetic storm were the root cause of the extreme weather in Greece, as we claimed in the case of the March 2012 heat wave in the USA [4]. It is worth noting that other satellites, like SOHO and PAMELA, measuring protons at high energies, recorded protons with spectrum extending much above 500 MeV [86,96]. In particular, it is of high importance the fact that the periods with rainfall in Alexandroupoli in early March started after solar cosmic ray streaming observed by SOHO, while between 3–31 March, the temperature in Alexandoupoli and the ACE/EPAM solar high energy (1.88–4.70 MeV) proton flux were strongly anticorrelated (r = −0.75, p = 0.05) (Point #9).

Visbeck et al. found that during a positive NAO (North Atlantic Oscillation), conditions are warmer and wetter than average in northern Europe, the eastern United States, and parts of Scandinavia, whereas conditions are colder and drier than average over the northwestern Atlantic and Mediterranean regions [97,98]. In [4] we argued that the positive NAO mediated the effect of the SEP event on the March 2012 heatwave in USA. Since the March 2012 bad weather in northeast Greece was an aspect of a large-scale weather activity including a region from the west Mediterranean/west Atlantic to the Middle East (Point #8; Figure 6) it is possible that positive NAO might be hypothesized to be responsible for the east Mediterranean/Aegean Sea fast airflow recorded after the major SEP event on 8–10 March 2012. However, other physical mechanisms cannot be excluded. For instance, the unusual the unusual strong energetic electron precipitation in the cusp (Figure 4) may also influenced the AEF fluctuation and bad weather on 8–10 and 11–12 March, 2012 in Xanthi (Thrace) [75]. Definitely, the possible relationship of NAO with atmospheric conditions in Greece and the east Mediterranean is an important topic for further research.

Finally, we should point out that our study on March 2012 weather in Thrace revealed variations in electric conditions. In particular we confirmed the presence of two types of electric disturbances at those times: (i) large amplitude atmospheric electric field variations at the beginning of rainfall on 8 March and 11 March (Point 4), and (ii) voltage variations in the electric power network in Thrace on 10 March 2012, during the decay phase of the magnetic storm [Point #11].

4.2. Sudden Voltage Changes on the Electric Power Grid in Thrace, Greece, in March 2012

Voltage anomalies were recorded in the electric grid in Thrace, Greece, during the magnetic storm on 7 March 2012 and during the recovery phase of the major storm on 10 and 11 March. The abrupt voltage variations in the electric grid in Thrace at a time period following the arrival of a greatly geoeffective ICME on 7 March and its associated SEP event on 7–9 March, should be understood as a result of the slowly varying geomagnetic field and the induced electric currents at those times (Figures 3 and 13).

Problems in transformers and electric grids as a result of some intense solar flares and ICMEs is a phenomenon that has attracted the interest of space research and remote sensing space weather research has been used to predict possible dangerous geoffective effects and protect human societies and technical systems. To this end several states have established special organizations or supported institutional research on GIC and their impact on power networks. For instance, the United States has supported this kind of research with the Federal Energy Regulatory Commission, the National Space Weather Strategy and the National Space Weather Action Plan [National Science and Technology Council, 2015]. In Australia the Power Transmission Network Service Providers cooperated with the Australian Energy Market Operator and the Australian Bureau of Meteorology to install some equipment to record GIC effects on some transformers in the Australian electric network [99]. The GICs constitute the space weather element in the National Risk Registry of the United Kingdom [100].

Many other states or individual researchers have conducted systematic research on GIC effects on electric networks at high, middle and low latitudes, as in New Zealand [101], South Africa [102–104], China [105,106], Brazil [107], Malaysia [108], Uruguay [109]. Similar studies have also been conducted in Mexico [110], Spain [111], Portugal [112] and Ethiopia [113].

Furthermore, the ACE and SOHO satellites located at the Lagrangian point L1 between the Sun and Earth as well as the observations of the Sun by space-based telescopes (i.e., AIA instrument on the SDO satellite used in the present study) have been extensively used to detect space weather and predict unusual magnetospheric and atmospheric phenomena. In addition, NOAA provides almost real-time data from ACE, which includes information ~1 h before the time that an intense ICME can cause catastrophic GIC effects on electric networks. Solar, space and ground measurements are combined to predict dangerous space weather conditions and protect electric networks. Ref. [114] has pointed out that medium GICs can provoke premature aging of the equipment of high voltage transformer. We should point out that there is good evidence that the voltage anomalies recorded in northeast Greece in March 2012 were related to the magnetic field variation during the storms of the 7 and 9–11 March. Firstly, at those times, no lightning activity was recorded in Thrace, Greece; secondly, the intense solar particle streaming, which was most probably the triggering agent of the meteorological extreme in the period after the ICME arrival at Earth on 7–9 March 2012, was not the cause of the voltage disturbances in the electric grid. This conclusion is supported by the fact that the highest occurrence frequency of SVCs were recorded on 10–11 March 2012, which is much later than the high energy solar particle flux maximum on 8 March 2012 (Figure 3c). Since the SVCs in Thrace were recorded during the two major storms in March 2012 (7 and 9 to 11), the SVCs can be attributed to the magnetic storm activity. Therefore, we claim that we can separate the different **drivers** of the March 2012 extreme meteorological events and of the voltage anomalies in the electric power grid in Thrace, Greece, in the course of ICME interaction with the Earth's physical/technological environment.

Two mechanisms can cause changes in the high voltage of the 150 kV transmission network: (1) the generation of voltage drops caused by arcing between high voltage lines and the Earth, as result of short-circuits, and voltage crossing to the Earth, due to the varying magnetic field during storms between the high voltage lines and the Earth, (2) surges creation (anomalous voltage increases), due to penetration of DC currents created by a CME-induced storm and consequently diffused from the ground into the transformers of the high voltage electric power grid [9].

It is possible that the large number of voltage drops that appeared on 7 and 10–11 March 2012 in the electric grid of Thrace, Greece, operating by the IPTO factory in Komotini, is due to high voltage arcs from cables to Earth or other conductive elements. These voltages arcs from cables to Earth may result either from an increase of magnetic field between cables and Earth or from an increase in the Earth's electric field. Any voltage arcing from cables to Earth, depending on the current passed to the Earth, is capable of causing the recorded voltage drops. The surges might be resulted from increase in storm induced quasi-DC electric field at Earth, through which the transmitted current is likely to have affected the high-voltage transformers, with the mechanism explained in Appendix E (Figure A2).

It is worth noting that many more sudden disturbances in the electric grid in Thrace occurred during the recovery phase of the March 2012 storm (Figures 10 and 11), which may suggest a preference for this phenomenon for slowly varying (quasi-DC) fields. A similar pattern can also be seen in the cases of the Geomagnetically Induced Currents estimated during the August and November 2018 magnetic storms recently studied by Hughes et al. [115] (their Figures 3 and 14).

Our finding is also consistent with the results of Zois [116] who investigated for the first time the effects of solar activity on the large transformers (150 kV and 400 kV) of the Greek national electric grid and he found preferential presence in transformer failures some (4–7) days after a geomagnetically stormy day.

Gil et al. (2023) pointed out recently that the Quebec blackout on 13 March 1989, has made GIC research a socially important field of study [117]. These authors concentrated on the fact that space weather may affect the power infrastructure not only at high latitudes but also in countries at lower latitudes. They considered the impact of the GIC on transformers and transmission lines in Greece, Spain, Italy, Slovakia, the Czech Republic, Austria, and Poland and conducted a statistical analysis that associates the total sum of the recorded transformer failures with the solar activity; they claimed that the mid-latitude countries could be actually under GIC impact during large geomagnetic storms.

The main emphasis in the studies examining the relation between solar and space weather activity and the space weather effects on technical infrastructure, has been given to failures of large transformers and electrical and electronic devices so far. Furthermore, there has also been some interest in the events on the power lines themselves, such as the repeated unplanned switching and power cuts. These events on the power lines have attracted only minimal interest so far.

The grid event records was considered so far as a minor component among several other failures in the research studies invstigating space weather effects on the whole electric power system. For instance, in a study of 12 years on the relationship between the anomalies of the grid components and the increased geomagnetic activity in the Czech Republic, the number of space weather-related events was estimated to be usually a few hundred per year [118]. In this study, the power line events were a small fraction of all types of failures, such as transformers, electrical substations, equipment etc. This approach implies that the power line events were a small fraction of the few hundred/year of the whole number of events. A small number of a few hundred of events suggests an occurrence frequency $f'_{SW} \approx 1$ event/day on average. The research conducted in the present study revealed ~135 events/11 days or an occurrence frequency $N_{SW} \approx 28$ events/day or $n \approx$ ~12 events/day on average. The vast difference between the occurrence of the events considered in the two studies manifests that our case study focused only on SVCs during a specific period with moderate geomagnetic activity is of a different nature from the previous ones and demonstrate the novelty of the methodology used.

The present study is the first one, which elaborates systematically on small short term (#sec) voltage fluctuations in an electrical power network. We point out that our methodology was based on analysising a continuous output of SVC data from the Independent Power Transmission Operator, in Komotini, northeast Greece, during times of moderate geomagnetic activity (Dst = -145 nT). We hypothesize that larger magnetic storms may cause more severe disturbances in the power grid in Thrace. Definitely, we infer that more studies are needed to check whether the continuous monitoring of SVCs might be used, not only to confirm, but also to forecast dangerous storm effects on the network under different space weather conditions.

We point out that the study of SVCs we performed in this paper is a direct manifestation of GICs and their frequency and the amplitude of the voltage fluctuations. Thus, since the GICs constitute the sole space weather element in the risk registry, this study suggest that SVC recording might be an independent and supplementary tool to GIC for power networks failure forecasting.

5. Conclusions

The influence of solar activity on Earth's climate is a well-known phenomenon [1,2,11,19,119,120]. Most studies have been devoted so far to investigate the solar cycle effects on the ionosphere, the stratosphere and the troposphere, while only a few case studies have been published examining the short-time effects of solar activity on atmospheric dynamics and the weather extremes.

Echer et al. found a very significant correlation ($r \approx 0.6$–0.8) between the sunspot number and the latitudinal averaged surface temperatures in the ~22 year-solar cycle [121]. However, there is good evidence that the solar activity produces different surface temperature responses at different latitudes and longitudes [33,37,122]. Therefore, different weather (i.e., temperature) responses to strong solar activity are expected.

In this perspective, we extended our previous study [4] on the possible causal relation between the unusual space weather variations and the famous March 2012 heatwave in America, by comparing the solar/space weather variations with the bad weather in Thrace, Greece, for the same time period (March 2012). To this end, we compared data from a large number of remote sensing experiments and we investigated physical processes in March 2012 on the Sun, the Interplanetary Space, the Earth's magnetosphere, the top of the clouds and the near-ground atmosphere.

The comparison of this extensive variety of data, all the way from the Sun to the Earth's ground, allowed us to conclude that there is good evidence of the influence of the unusual geoeffective solar activity and space weather conditions between 6–14 March 2012 [14,118] on the extreme weather events in Thrace, Greece. Here, it is worth noting the impressive information given by an ESA report: «Already in ancient Greece, around 400 B.C., Meton observed sunspots (Hoyt and Schatten, 1997). After twenty years of solar studies he came to the conclusion that solar activity, i.e., high number of sunspots, is associated with wet weather in Greece. Today the observations of Meton could have been associated with the changes of the North Atlantic Oscillation (NAO) (Hurrell et al., 2003)» [123]. Indeed, the March 2012 bad weather in Greece occurred during times of increased positive NAO index [4] (Figure 5).

The analysis of data demonstrated that the winter-like weather in Thrace on 7–14 March was an aspect of large scale weather anomalies taking place all over the north Europe, the Mediterranean Sea, the southeast Europe, the Aegean Sea and the southeast European countries.

A comparison of the features of 28 large (<-150 nT) ICME-related magnetic storms during a period of ~18 years (1997–2015) implied the conclusion that the solar cosmic rays were most probably the root cause of the solar impact on the early March 2012 winter-like weather events in Thrace, Greece, as it was suggested in the study on March 2012 heatwave in USA [4], which started on the same day (6 March). This conclusion is in agreement with the results of Pudovkin and Raspopov [38] and Pudovkin and Babushkina [39], that the main extraterrestrial driver of weather variations in the lower atmosphere is the solar and galactic cosmic ray radiation.

The relationship between space and geophysical processes in two such distant regions on the planet, as the USA [4] and Greece (present study), strongly supports the hypothesis of the significant role of solar activity in triggering the low troposphere weather in March 2012 in Thrace, Greece. Furthermore, the fact that the space weather-related March 1910 and March 2012 heatwaves in the USA were an aspect of global atmospheric anomalies suggests that the special solar activity was most probably the root cause of the two historic events [124].

Our conclusion is that the March 2012 heatwave in the USA [4] and the winter-like weather in Greece at the same time period were the results of a common driver mechanism may have essential implications in fully understanding some of the weather changes and, therefore, it needs further examination, in particular in our times, when the frequency of extreme weather events has been increased. The need for estimating anthropogenic versus physical contribution in climate change appears to be of the highest importance. Furthermore, the results of the present paper suggest that detailed case studies based on multi-instrument high-time (i.e., #min/h/day) resolution data are essential in extracting hidden information from extreme weather events.

Furthermore, we reported, for the first time, the results of a systematic study of sudden (within 1 s) voltage changes in an electric power network at middle latitudes, namely in the power network of Thrace/Greece, located at ~41°N, during times of a series of moderate to intense magnetic storms (5–15 March 2012). During the March 2012 magnetic storm important voltage changes in the electric grid were recorded during the decay phase. Although the amplitude of the voltage fluctuations was rather small (maximum voltage surge at 3.61 kV and voltage drop at -3.32 kV on March 10), this effect may be important under different geomagnetic/geophysical conditions and in higher latitude electric power grids.

As an epilogue, we could comprehensively describe the contribution of the present paper to the Space based research on extreme weather events in the words of one of the reviewers of the present paper: "The study utilizes a wide range of data from a wide range of remote sensing techniques in order to discover the root cause of the extreme weather that unfolded in Greece in March 2012 and also the resultant impact ιn power grids. One of the novel findings is the documentation of geomagnetically induced voltage changes in electric grids. The obtained improved understanding opens a new window into space weather applications research. This is a significant addition to the field, since the existing gap and lack of knowledge along with the absence of sufficient information in this field are created by the limited studies researching the root cause of climate change that is widely attributed to human activity".

Author Contributions: Conceptualization, G.A. and A.K. (Anastasios Karkanis); methodology, G.A. and A.K. (Anastasios Karkanis); software, A.K. (Anastasios Karkanis), S.-A.M., D.O. and N.H.; validation, G.A. and M.D.; formal analysis, G.A., S.-A.M., P.M. and S.K.; investigation, G.A., A.K. (Anastasios Karkanis), D.E., S.K. and D.O.; data curation, A.K. (Athanasios Kampatagis), A.K. (Anastasios Karkanis), G.A., S.-A.M., D.O., S.K. and N.H.; writing—original draft preparation, G.A., A.K. (Anastasios Karkanis) and P.M.; writing—review and editing, G.A., D.E., P.M., A.K. (Anastasios Karkanis) and M.D.; visualization, A.K. (Anastasios Karkanis), S.-A.M., D.O. and N.H.; supervision, G.A. and M.D.; funding acquisition, G.A. All authors have read and agreed to the published version of the manuscript.

Funding: This research received no external funding.

Data Availability Statement: ACE/EPAM data are available here: http://www.srl.caltech.edu/ACE/ASC/level2/lvl2DATA_EPAM.html (accessed on 17 December 2023). More information on the data used in this study are mentioned in the "Acknowledgments" section.ow.

Acknowledgments: The first author (G.A.) thanks L. Lanzerotti for providing the ACE/EPAM energetic particle data as well as K. Kourtidis for providing meteorological data (Figure 8) from the Laboratory of Air Pollution and Pollution Control Engineering of Atmospheric Pollutants, Dept. of Environmental Engineering, Democritus University of Thrace, Xanthi, Greece, and TERRA/MODIS data processing as well as V. Kotroni for helping us to extract useful information from the National Observatory of Athens / ZEUS LITHTNING DATA. G.A. also thanks K. Kourtidis for helpful discussions and his comments on a preliminary version of the present manuscript. The authors acknowledge the use of data from: the Weather Online Services (1), the World Data Center for Geomagnetism, Kyoto (2), AIA instrument onboard the SDO satellite from helioviewer.org/ (3), the MODIS (Moderate Resolution Imaging Spectroradiometer) instrument on the satellites TERRA and AQUA, produced with the Giovanni online data system, developed and maintained by the NASA GES DISC (4) NOAA**,** NCEP (National Centers for Environmental Prediction) and (5) and NOAA satellites (NOAA 18/19). 1. http://www.weatheronline.co.uk/weather/maps/forecastmaps?LANG=en&CONT=ukuk&R=150; accessed on 5 October 2023; 2. https://wdc.kugi.kyoto-u.ac.jp/dstdir; accessed on 5 October 2023, 3. https://helioviewer.org/, 4. https://giovanni.gsfc.nasa.gov/giovanni/; accessed on 10 October 2023 5. https://www.weather.gov/ncep/; 20 March 2014.

Conflicts of Interest: The remaining authors declare that the research was conducted in the absence of any commercial or financial relationships that could be construed as a potential conflict of interest.

Appendix A

Table A1. Cross-correlation results between the temperature in Alexandoupoli T_A and the ACE/EPAM P8 high energy (1.88–4.70 MeV) proton flux P8 for lags k = −3, . . .0, . . ., 3.

Lag P8—T_A	CC
−3	−0.6446
−2	−0.7059
−1	−0.7296
0	−0.7504
1	−0.7369
2	−0.7114
3	−0.6680

Appendix B

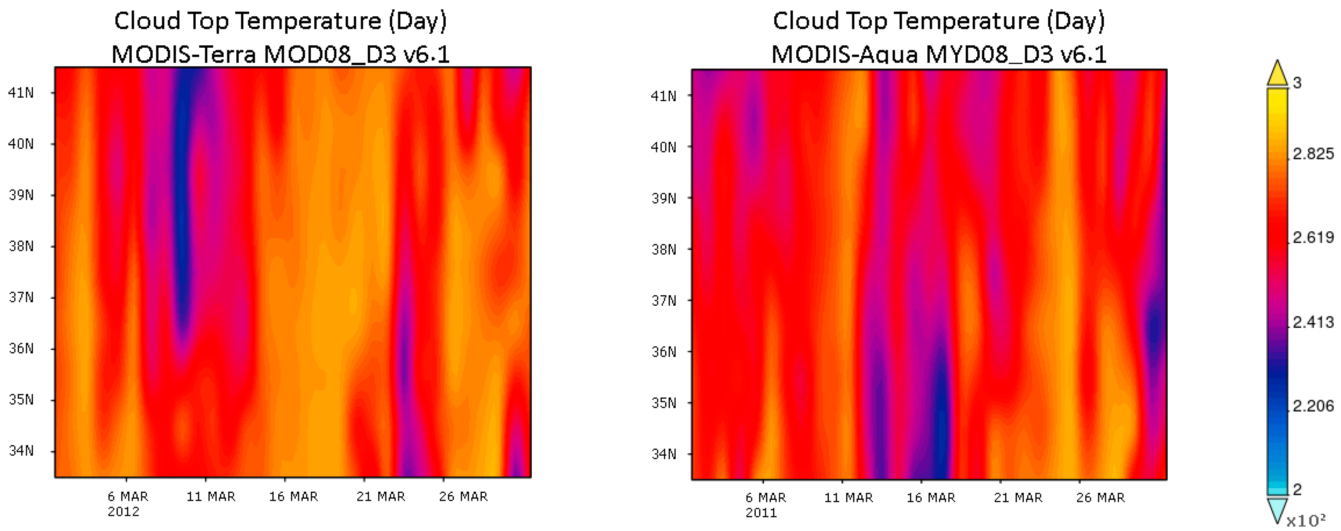

Figure A1. Data in the same format as in Figure 5, but for a year before (March 2011). MODIS CTT apps for the same region as in Figure 5 show no similarities to the 2012 MODIS CTT.

Appendix C

The detection of sudden voltage variations (voltage increase and voltage decrease) was achieved according to the algorithm:

$$\Delta V_n = V_n - (V_n + V_{n-1} + V_{n-2} + V_{n-3} + V_{n-4}\ V_{n-5})/5 \quad \text{(A1)}$$

where, $\Delta V_n > 0.5$ kV (for voltage increase) or $\Delta V_n < -0.5$ kV (for voltage decrease).

Appendix D

Table A2. The number of SVC events Nsvc and the number of assumed magnetic storm-related SVC events, between 5–15 March 2012. The number of sudden voltage drops and surges created in the electric power in Thrace, Greece, was highest on 10 March 2012, during the decay phase of the major magnetic storm in March 2012 (Figures 3 and 13). In addition, the highest value (3.61 kV) of the sudden voltage drop and the surges creation was recorded on the same day.

Date	# SVC Events (Nsvc)	# Storm-Related SVC	Maximum Surges Creation (kV)	Maximum Voltage Drop (kV)
5 March 2012	7	2	0.89	−0.66
6 March 2012		15	0.75	−0.73
7 March 2012	22	16	1.47	−1.08
8 March 2012	25	16	1.19	−0.91
9 March 2012	24	18	0.71	−0.72
10 March 2012	37	28	3.61	−3.32
10 March 2012	16	16	0.61	−0.63
12 March 2012	6	6	0.00	−0.67
13 March 2012	9	2	0.58	−0.67
14 March 2012	12	8	1.08	−0.85
15 March 2012	23	9	0.80	−1.11

Appendix E

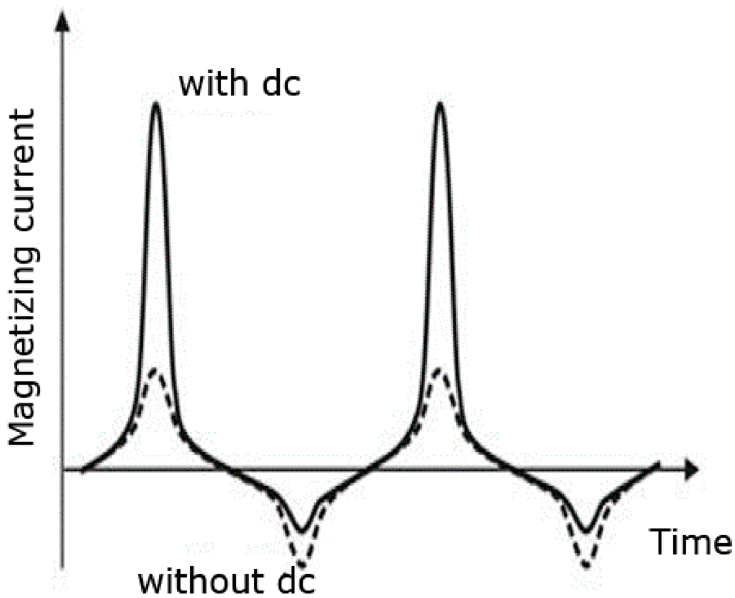

Figure A2. Surges creation due to penetration of DC current caused by an ICME are diffused from the ground into the transformers of the high voltage grid. The larger the DC current that can be added to the AC of a coil, the more deformation is caused and the waveform of the transformer's current is more asymmetric. Figure A2 shows that the the positive AC waveform amplitudes are five times higher due to the effect of the DC [30].

References

1. Shindell, D.T.; Schmidt, G.A.; Mann, M.E.; Rind, D.; Waple, A. Solar Forcing of Regional Climate Change during the Maunder Minimum. *Science* **2001**, *294*, 2149–2152. [CrossRef]
2. Easterbrook, D. *The Solar Magnetic Cause of Climate Changes and Origin of the Ice Ages*, 3rd ed.; Independently Publisher: Washington, DC, USA, 2019.
3. Avakyan, S.V.; Voronin, N.A.; Nikol'sky, G.A. Response of Atmospheric Pressure and Air Temperature to the Solar Events in October 2003. *Geomagn. Aeron.* **2015**, *55*, 1180–1185. [CrossRef]
4. Anagnostopoulos, G.C.; Menesidou, S.-A.I.; Efthymiadis, D.A. The March 2012 HeatWave in Northeast America as a Possible Effect of Strong Solar Activity and Unusual Space Plasma Interactions. *Atmosphere* **2022**, *13*, 926. [CrossRef]
5. Coumou, D.; Rahmstorf, S. A Decade of Weather Extremes. *Nat. Clim. Change* **2012**, *2*, 491–496. [CrossRef]
6. Robine, J.-M.; Cheung, S.L.K.; Roy, S.L.; Oyen, H.V.; Griffiths, C.; Michel, J.-P.; Herrmann, F.R. Death Toll Exceeded 70,000 in Europe during the Summer of 2003. *Comptes. Rendus. Biol.* **2008**, *331*, 171–178. [CrossRef]
7. CarbonBrief, Attributing Extreme Weather to Climate Change. Available online: https://www.carbonbrief.org/mapped-howclimate-change-affects-extreme-weather-around-the-world (accessed on 1 March 2022).
8. Dole, R.; Hoerling, M.; Perlwitz, J.; Eischeid, J.; Pegion, P.; Zhang, T.; Quan, X.-W.; Xu, T.; Murray, D. Was There a Basis for Anticipating the 2010 Russian HeatWave? *Geophys. Res. Lett.* **2011**, *38*, L06702. [CrossRef]
9. Kumar, A.S.; Chen, M.; Hoerling, M.; Eischeid, J. Do Extreme Climate Events Require Extreme Forcings. *Geophys. Res. Lett.* **2013**, *40*, 3440–3445. [CrossRef]
10. Love, J.; Hayakawa, H.; Cliver, E. On the Intensity of the Magnetic Superstorm of September 1909. *Space Weather.* **2019**, *17*, 37–45. [CrossRef]
11. Connolly, R.; Soon, W.; Connolly, M.; Baliunas, S.; Berglund, J.; Butler, C.J.; Cionco, R.G.; Elias, A.G.; Fedorov, V.M.; Harde, H.; et al. How Much Has the Sun Influenced Northern Hemisphere Temperature Trends? An Ongoing Debate. *Res. Astron. Astrophys.* **2021**, *21*, 131. [CrossRef]
12. Hundhausen, A.J. *Coronal Expansion and Solar Wind*; Springer: New York, NY, USA, 1972.
13. Richardson, I.G. Solar wind stream interaction regions throughout the heliosphere. *Liv. Rev. Sol. Phys.* **2018**, *1*, 15. [CrossRef]
14. Patsourakos, S.; Georgoulis, M.K.; Vourlidas, A.; Nindos, A.; Sarris, T.; Anagnostopoulos, G.C.; Anastasiadis, A.; Chintzoglou, G.; Daglis, I.A.; Gontikakis, C.; et al. The major geoeffectiveSolar eruptions of 2012 March 7: Comprehensive Sun-to-Earth analysis. *Astrophys. J.* **2016**, *817*, 14. [CrossRef]
15. Barnes, A. *Solar-Terrestrial Physics: Principles and Theoretical Foundations*; Carovillano, R.L., Forbes, J.M., Eds.; D. Reidel Publishing Company: Dordrecht, The Netherlands, 1983; pp. 155–199.
16. Kumar, A.; Badruddin, B. Study of the evolution of the geomagnetic disturbances during the passage of high-speed streams from coronal holes in solar cycle 2009–2016. *Astrophys. Space Sci.* **2021**, *366*, 21. [CrossRef]
17. Abdu, M.A.; de Souza, J.R.; Sobral, J.H.A.; Batista, I.S. Magnetic Storms Associated Disturbance Dynamo Effects in the Low and Equatorial Latitude Ionosphere. *Recurr. Magn. Storms Corotating Sol. Wind. Streams Geophys. Monogr. Ser.* **2006**, *167*, 283–304. [CrossRef]
18. Prikryl, P.; Ghoddousi-Fard, R.; Thomas, E.G.; Ruohoniemi, J.M.; Shepherd, S.G.; Jayachandran, P.T.; Danskin, D.W.; Spanswick, E.; Zhang, Y.; Jiao, Y.; et al. GPS phase scintillation at high latitudes during geomagnetic storms of 7–17 March 2012—Part 1: The North American sector. *Ann. Geophys.* **2015**, *33*, 637–656. [CrossRef]
19. Gray, L.J.; Beer, J.; Geller, M.; Haigh, J.D.; Lockwood, M.; Matthes, K.; Cubasch, U.; Fleitmann, D.; Harrison, G.; Hood, L.; et al. Solar Influence on Climate. *Rev. Geophys.* **2010**, *48*, RG4001. [CrossRef]
20. Herman, J.R.; Goldberg, R.A. *Sun Weather and Climate*; Dover Pub Inc.: New York, NY, USA, 1978.
21. Anagnostopoulos, G.C.; Spyroglou, I.; Rigas, A.; Preka-Papadema, P.; Mavromichalaki, H.; Kiosses, I. The sun as a significant agent provoking earthquakes. *Eur. Phys. J. Spec. Top.* **2021**, *230*, 287–333. [CrossRef]
22. Anagnostopoulos, G.C.; Papandreou, A. Space conditions during a month of a sequence of six M > 6.8 earthquakes ending with the tsunami of 26 December 2004. *Nat. Hazards Earth Syst. Sci.* **2012**, *12*, 1551–1559. [CrossRef]
23. Duma, G.; Ruzhin, Y. Diurnal changes of earthquake activity and geomagnetic Sq-variations. *Nat. Hazards Earth Syst. Sci.* **2003**, *3*, 171–177. [CrossRef]
24. Zenchenko, T.A.; Breus, T.K. The Possible Effect of Space Weather Factors on Various Physiological Systems of the Human Organism. *Atmosphere* **2021**, *12*, 346. [CrossRef]
25. Venclovienе, J.; Babarskiene, R.; Slapikas, R. The association between solar particle events, geomagnetic storms, and hospital admissions for myocardial infarction. *Nat. Hazards* **2013**, *65*, 1–12. [CrossRef]
26. Noula, M.; Preka-Papadema, P.; Moussas, X.; Vassiliou, C.; Tsaliki, S.-M.; Kontogeorgou, E.; Katsavrias, C.; Theodoropoulou, A. Recorded Cases at the Emergency Department of the General Hospital of Lamia Town during the Year 2005 in Association with Helio-geomagnetic Activity. *Hell. J. Nurs. Sci.* **2010**, *3*, 53–62.
27. Palmer, S.J.; Rycroft, M.J.; Cermack, M. Solar and geomagnetic activity, extremely low frequency magnetic and electric fields and human health at the Earth's surface. *Surv. Geophys.* **2006**, *27*, 557–595. [CrossRef]
28. Lanzerotti, L.J. Space Weather: Historical and Contemporary Perspectives. *Space Sci. Rev.* **2017**, *212*, 1253–1270. [CrossRef]
29. Marhavilas, P.K. The Space Environment and its Impact on Human Activity. CSEG RECORDER. *Can. Soc. Explor. Geophys.* **2004**, *29*, 41–50.

30. Kirkham, H.; Makarov, Y.V.; Dagle, J.E.; DeSteese, J.G.; Elizondo, M.A.; Diao, R. *Geomagnetic Storms and Long-Term Impacts on Power Systems*; Pacific Northwest National Laboratory: Richland, WA, USA, 2011. [CrossRef]
31. Labitzke, K.; Kunze, M.; Brönnimann, S. Sunspots, the QBO and the Stratosphere in the North Polar Region 20 Years Later. *Meteorol. Z.* **2006**, *15*, 355–363. [CrossRef]
32. Raspopov, O.; Veretenenko, S. Solar Activity and Cosmic Rays: Influence on Cloudiness and Processes in the Lower Atmosphere (in Memory and on the 75th Anniversary of M.I. Pudovkin). *Geomagn. Aeron.* **2009**, *49*, 137–145. [CrossRef]
33. Schuurmans, C.J.E. Tropospheric Effects of Variable Solar Activity. *Sol. Phys.* **1981**, *74*, 417–419. [CrossRef]
34. Pudovkin, M.I. Influence of Solar Activity on the Lower Atmosphere State. *Int. J. Geomagn. Aeron.* **2004**, *5*, GI2007. [CrossRef]
35. Siingh, D.; Singh, R.P.; Singh, A.K.; Kulkarni, M.N.; Gautam, A.S.; Singh, A.K. Solar Activity, Lightning and Climate. *Surv. Geophys.* **2011**, *32*, 659–703. [CrossRef]
36. Le Mouël, J.-L.; Lopes, F.; Courtillot, V.A. Solar Signature in Many Climate Indices. *J. Geophys. Res. Atmos.* **2019**, *124*, 2600–2619. [CrossRef]
37. Kossobokov, V.; Mouël, J.L.; Courtillot, V. On the Diversity of Long-Term Temperature Responses to Varying Levels of Solar Activity at Ten European Observatories. *Atmos. Clim. Sci.* **2019**, *9*, 498–526. [CrossRef]
38. Pudovkin, M.I.; Raspopov, O.M. A mechanism of solar activity influence on the state of the lower atmosphere and meteoparameters. *Geomagn. Aeron.* **1992**, *32*, 1–9.
39. Pudovkin, M.I.; Babushkina, S.V. Influence of Solar Flares and Disturbances of the Interplanetary Medium on the Atmospheric Circulation. *J. Atmos. Terr. Phys.* **1992**, *54*, 841–846. [CrossRef]
40. Smirnov, S.E.; Mikhailova, G.A.; Kapustina, O.V. Variations in Electric and Meteorological Parameters in the Near-Earth's Atmosphere at Kamchatka during the Solar Events in October 2003. *Geomagn. Aeron.* **2014**, *54*, 240–247. [CrossRef]
41. Mironova, I.A.; Usoskin, I.G. Possible Effect of Strong Solar Energetic Particle Events on Polar Stratospheric Aerosol: A Summary of Observational Results. *Environ. Res. Lett.* **2014**, *9*, 015002. [CrossRef]
42. Tinsley, B.A.; Deen, G.W. Apparent Tropospheric Response to MeV-GeV Particle Flux Variations: A Connection via Electrofreezing of Supercooled Water in High-Level Clouds? *J. Geophys. Res.* **1991**, *96*, 22283–22296. [CrossRef]
43. Marsh, N.; Svensmark, H. Cosmic Rays, Clouds, and Climate. *Space Sci. Rev.* **2000**, *94*, 215–230. [CrossRef]
44. Roldugin, V.; Tinsley, B.A. Atmospheric Transparency Changes Associated with SolarWind-Induced Atmospheric Electricity Variations. *J. Atmos. Sol.-Terr. Phys.* **2004**, *66*, 1143–1149. [CrossRef]
45. Bazilevskaya, G.A.; Usoskin, I.G.; Flückiger, E.O.; Harrison, R.G.; Desorgher, L.; Bütikofer, R.; Krainev, M.B.; Makhmutov, V.S.; Stozhkov, Y.I.; Svirzhevskaya, A.K.; et al. Cosmic Ray Induced Ion Production in the Atmosphere. *Space Sci. Rev.* **2008**, *137*, 149–173. [CrossRef]
46. Boteler, D.H. *Space Weather Effects on Power Systems*; Song, P., Singer, H.J., Siscoe, G.L., Eds.; Space Weather Geophysical Monograph Series; AGU: Washington, DC, USA, 2001; Volume 125, pp. 347–352.
47. Kappenman, J. Geomagnetic Storms and Their Impacts on the U.S. Power Grid. Metatech Corporation, Goleta, Calif 93117. January 2010. Available online: http://web.ornl.gov/sci/ees/etsd/pes/pubs/ferc_Meta-R-319.pdf (accessed on 26 July 2015).
48. Kappenman, J.G. The Evolving Vulnerability of Electric Power Grids. *Space Weather* **2004**, *2*, 1. [CrossRef]
49. Kappenman, J.G.; Albertson, V.D. Bracing for the geomagnetic storms. *IEEE Spectr.* **1990**, *27*, 27–33. [CrossRef]
50. Kappenman, J.G. *Advanced Geomagnetic Storm Forecasting for the Electric Power Industry*; Song, P., Singer, H.J., Siscoe, G.L., Eds.; Space Weather Geophysical Monograph Series; AGU: Washington, DC, USA, 2001; Volume 125, pp. 353–358. [CrossRef]
51. Thomson, A. Space Weather and Power Grids. Earthwise 2010, 26, British Geological Survey, NERC. Available online: https://geomag.bgs.ac.uk/documents/Earthwise_26_powergrids.pdf (accessed on 2 October 2023).
52. Liu, J.; Wang, C.B.; Liu, L.; Sun, W.-H. The response of local power grid at low-latitude to geomagnetic storm: An application of the Hilbert Huang transform. *Space Weather* **2016**, *14*, 300–312. [CrossRef]
53. Nicoll, K.A. Space weather influences on atmospheric electricity. *Weather* **2014**, *69*, 238–241, ISSN 1477-8696. [CrossRef]
54. American Meteorological Society, Glossary of Meteorology. Available online: https://glossary.ametsoc.org/wiki/Atmospheric_electric_field (accessed on 2 October 2023).
55. Bennett, A.J.; Harrison, R.G. Variability in surface atmospheric electric field measurements. *J. Phys. Conf. Ser.* **2008**, *142*, 012046. [CrossRef]
56. Li, L.; Chen, T.; Ti, S.; Wang, S.-H.; Song, J.-J.; Cai, C.-L.; Liu, Y.-H.; Li, W.; Luo, J. Fair-Weather Near-Surface Atmospheric Electric Field Measurements at the Zhongshan Chinese Station in Antarctica. *Appl. Sci.* **2022**, *12*, 9248. [CrossRef]
57. Troshichev, O.A.; Frank-Kamenetsky, A.; Burns, G.; Fuellekrug, M.; Rodger, A.; Morozov, V. The relationship between variations of the atmospheric electric field in the southern polar region and thunderstorm activity. *Adv. Space Res.* **2004**, *34*, 1801–1805. [CrossRef]
58. Whipple, F.J.W. Modern views on atmospheric electricity. *Q. J. R. Meteorol. Soc.* **2007**, *64*, 199–222. [CrossRef]
59. Liu, C.; Williams, E.R.; Zipser, E.J.; Burns, G. Diurnal Variations of Global Thunderstorms and Electrified Shower Clouds and Their Contribution to the Global Electrical Circuit. *J. Atmos. Sci.* **2010**, *67*, 309–323. [CrossRef]
60. Tinsley, B.A.; Burns, G.B.; Zhou, L. The role of the global electric circuit in solar and internal forcing of clouds and climate. *Adv. Space Res.* **2007**, *40*, 1126–1139. [CrossRef]
61. Telang, A.V.R. The influence of rain on the atmospheric-electric field. *J. Geophys. Res.* **1930**, *35*, 125–131. [CrossRef]
62. Yan, M.; Shen, Q.; Zhou, C. Atmospheric electric field at ground in partial region in China. *Plateau Meteorol.* **1988**, *2*, 156–165.

63. Tacza, J.; Raulin, J.P.; Mendonça, R.; Makhmutov, V.; Marun, A.; Fernandez, G. Solar Effects on the Atmospheric Electric Field During 2010–2015 at Low Latitudes. *J. Geophys. Res. Atmos.* **2018**, *123*, 11–970. [CrossRef]
64. Zhang, H.; Zhang, Y.; Yang, S. Characteristics of atmospheric electric field in Taiyuan and its relationship with atmospheric pollutants. *Environ. Sci. Technol.* **2013**, *36*, 66–69.
65. Li, J.; Chen, X.; Cheng, Y.; Li, R.; Dong, F. Preliminary Study on the Relationship between Atmospheric Electric Field and Air Pollutants in Beijing. *Plateau Weather* **2021**, *40*, 209–218.
66. Huang, Y.; Wu, A.; Zhang, S. Influence of environmental features on the atmospheric electric field and correction. *Electron. Meas. Technol.* **2018**, *41*, 35–38.
67. Gurmani, S.F.; Ahmad, N.; Tacza, J.; Iqbal, T. First seasonal and annual variations of atmospheric electric field at a subtropical station in Islamabad, Pakistan. *J. Atmos. Sol.-Terr. Phys.* **2018**, *179*, 441–449. [CrossRef]
68. Zhou, Y.; Chen, C.P.; Liu, L.P.; Chu, R.Z.; Feng, J.M.; Zhang, T.; Song, X.M.; Kajikawa, M.; Fujii, H.Y.; Aoi, T.; et al. Atmospheric electric field in hail weather system in Naqu area of Qinghai-Tibet Plateau. *Plateau Weather* **2000**, *3*, 339–347.
69. Zhang, Y.; Meng, Q. Atmospheric Electricity Characteristics in the Eastern Qinghai-Tibet Plateau. *Plateau Weather* **1998**, *17*, 135–141.
70. Yan, M.; Xiao, Q. Analysis of the characteristics of the atmospheric electric field in the western Pacific Ocean from September to November in 1988. *Plateau Weather* **1990**, *9*, 395–404.
71. Choudhury, A.; Guha, A.; De, B.K.; Roy, R. A statistical study on precursory effects of earthquakes observed through the atmospheric vertical electric field in northeast India. *Ann. Geophys.* **2013**, *56*, R0331.
72. Smirnov, S. Association of the negative anomalies of the quasistatic electric field in atmosphere with Kamchatka seismicity. *Nat. Hazards Earth Syst. Sci.* **2008**, *8*, 745–749. [CrossRef]
73. Chen, T.; Zhang, X.X.; Zhang, X.M.; Jin, X.B.; Wu, H.; Ti, S.; Li, R.K.; Li, L.; Wang, S.H. Imminent estimation of earthquake hazard by regional network monitoring the near surface vertical atmospheric electrostatic field. *Chin. J. Geophys.* **2021**, *64*, 1145–1154.
74. Pulinets, S.; Boyarchuk, K. *Ionospheric Precursors of Earthquakes*; Springer: Berlin, Germany, 2005; ISBN 978-3-540-26468-2.
75. Kleimenova, N.G.; Gromova, L.I.; Gromov, S.V.; Malysheva, L.M. Large Magnetic Storm on September 7–8, 2017: High-Latitude Geomagnetic Variations and Geomagnetic Pc5 Pulsations. *Geomagn. Aeron.* **2018**, *58*, 597–606. [CrossRef]
76. Michnowski, S.; Odzimek, A.; Kleimenova, N.G.; Kozyreva, O.V.; Kubicki, M.; Klos, Z.; Israelsson, S.; Nikiforova, N.N. Review of Relationships Between Solar Wind and Ground-Level Atmospheric Electricity: Case Studies from Hornsund, Spitsbergen, and Swider, Poland. *Surv. Geophys.* **2021**, *42*, 757–801. [CrossRef]
77. Pesnell, W.D.; Thompson, B.J.; Chamberlin, P.C. The Solar Dynamics Observatory (SDO). *Sol. Phys.* **2012**, *275*, 3–15. [CrossRef]
78. Stone, E.C.; Burlaga, L.F.; Cummings, A.C.; Feldman, W.C.; Frain, W.E.; Geiss, J.; Gloeckler, G.; Gold, R.E.; Hovestadt, D.; Krimigis, S.M.; et al. The Advanced Composition Explorer. *AIP Conf. Proc.* **1990**, *203*, 48–57.
79. EOS, NASA' Earth Observing System, Terra. Available online: https://eospso.nasa.gov/missions/terra (accessed on 29 November 2023).
80. NASA, Aqua Project Science. Available online: https://aqua.nasa.gov/content/about-aqua (accessed on 29 November 2023).
81. NASA, MODIS (Moderate Resolution Imaging Spectroradiometer). Available online: https://modis.gsfc.nasa.gov/ (accessed on 30 November 2023).
82. NS ENERGY, Komotini Combined-Cycle Power Plant. Available online: https://www.nsenergybusiness.com/projects/komotini-combined-cycle-power-plant/# (accessed on 30 November 2023).
83. World Data Center for Geomagnetism, Geomagnetic Equatorial Dst Index Home Page, Kyoto. Available online: https://wdc.kugi.kyoto-u.ac.jp/dstdir/ (accessed on 30 November 2023).
84. Tsurutani, B.T.; Echer, E.; Shibata, K.; Verkhoglyadova, O.P.; Mannucci, A.J.; Gonzalez, W.D.; Kozyra, J.; Pätzold, M. The Interplanetary Causes of Geomagnetic Activity during the 7–17 March 2012 Interval: A Cawses II overview. *J. Space Weather Space Clim.* **2014**, *4*, 8. [CrossRef]
85. Tsurutani, B.T.; McPherron, R.L.; Gonzalez, W.D.; Lu, G.; Gopalswamy, N.; Guarnieri, F.L. Magnetic Storms Caused by Corotating Solar Wind Streams, in Recurrent Magnetic Storms: Corotating Solar Wind. *Geophys. Monogr.* **2006**, *167*, 1. [CrossRef]
86. Maragkakis, M.G.; Anagnostopoulos, G.C.; Vassiliadis, E.S. Upstream Ion Events with Hard Energy Spectra: Lessons for Their Origin from a Comparative Statistical Study (ACE/Geotail). *Planet. Space Sci.* **2013**, *85*, 1–12. [CrossRef]
87. Kühl, P.; Dresing, N.; Heber, B.; Klassen, A. Solar Energetic Particle Events with Protons Above 500 MeV Between 1995 and 2015 Measured with SOHO/EPHIN. *Sol. Phys.* **2017**, *292*, 10. [CrossRef]
88. Papaioannou, A.; Souvatzoglou, G.; Paschalis, P.; Gerontidou, M.; Mavromichalaki, H. The First Ground-Level Enhancement of Solar Cycle 24 on 17 May 2012 and Its Real-Time Detection. *Sol. Phys.* **2014**, *289*, 423–436. [CrossRef]
89. Gurnett, D.A.; Kurth, W.S.; Burlaga, L.F.; Ness, N.F. In Situ Observations of Interstellar Plasma with Voyager 1. *Science* **2013**, *341*, 1489–1492. [CrossRef]
90. Zeitlin, C.; Hassler, D.M.; Cucinotta, F.A.; Ehresmann, B.; Wimmer-Schweingruber, R.F.; Brinza, D.E.; Kang, S.; Weigle, G.; Böttcher, S.; Böhm, E.; et al. Measurements of Energetic Particle Radiation in Transit to Mars on the Mars Science Laboratory. *Science* **2013**, *340*, 1080–1084. [CrossRef]
91. Dole, R.; Hoerling, M.; Kumar, A.; Eischeid, J.; Perlwitz, J.; Quan, X.-W.; Kiladis, G.; Webb, R.; Murray, D.; Chen, M.; et al. The making of an extreme event: Putting the Pieces Together. *Bull. Am. Meteorol. Soc.* **2014**, *95*, ES57–ES60. [CrossRef]

92. Hanna, J.; Schultz, D.; Irving, A. Cloud-Top Temperatures for Precipitating Winter Clouds. *J. Appl. Meteorol. Clim.* **2008**, *47*, 351–359. [CrossRef]
93. Kastelis, N.; Kourtidis, K. Characteristics of the atmospheric electric field and correlation with CO2 at a rural site in southern Balkans. *Earth Planets Space* **2016**, *68*, 3. [CrossRef]
94. Nicoll, K.; Harrison, R.G.; Bor, J.; Barta, V.; Brugge, R.; Chillingarian, A.; Chum, J.; Georgoulias, A.; Guha, A.; Kourtidis, K.; et al. A global atmosphereic electricity monitoring network for climate and geophysical research. *J. Atmos. Sol.-Terr. Phys.* **2019**, *184*, 18–29. [CrossRef]
95. Mikhailova, G.A.; Kapustina, O.V.; Smirnov, S.E. Effects of solar and geomagnetic activities in variations of power spectra of electrical and meteorological parameters in the near-Earth atmosphere in Kamchatka during October 2003 solar events. *Geomagn. Aeron.* **2014**, *54*, 645–654. [CrossRef]
96. Bazilevskaya, G.A.; Mayorov, A.G.; Mikhailov, V.V. Comparison of Solar Energetic Particle Events Observed by PAMELA Experiment and by Other Instruments in 2006–2012. In Proceedings of the International Cosmic Rays Conference, Rio de Janeiro, Brazil, 2–9 July 2013; Volume 33, p. 1392.
97. Woollings, T.; Lockwood, M.; Masato, G.; Bell, C.; Gray, L. Enhanced signature of solar variability in Eurasian winter climate. *Geophys. Res. Lett.* **2010**, *37*, L20805. [CrossRef]
98. Visbeck, M.H.; Hurrell, J.W.; Polvani, L.; Cullens, H.M. The North Atlantic Oscillation: Past, present, and future. *Proc. Natl. Acad. Sci. USA* **2001**, *98*, 12876–12877. [CrossRef] [PubMed]
99. Marshall, R.A.; Kelly, A.; Van Der Walt, T.; Honecker, A.; Ong, C.; Mikkelsen, D.; Spierings, A.; Ivanovich, G.; Yoshikawa, A. Modeling geomagnetic induced currents in Australian power networks. *Space Weather* **2017**, *15*, 7. [CrossRef]
100. Cabinet Office; National Risk Register of Civil Emergencies. 2015. Available online: https://assets.publishing.service.gov.uk/government/uploads/system/uploads/attachment_data/file/419549/20150331_2015-NRR-WA_Final.pdf (accessed on 2 October 2023).
101. Divett, T.; Richardson, G.S.; Beggan, C.D.; Rodger, C.J.; Boteler, D.H.; Ingham, M.; MacManus, D.H.; Thomson, A.W.P.; Dalzell, M. Transformer-level modeling of geomagnetically induced currents in New Zealand's South Island. *Space Weather* **2018**, *16*, 718–735. [CrossRef]
102. Koen, J.; Gaunt, T. Geomagnetically induced currents in the Southern African electricity transmission network. In Proceedings of the 2003 IEEE Bologna Power Tech Conference Proceedings, Bologna, Italy, 23–26 June 2003; p. 7.
103. Gaunt, C.T.; Coetzee, G. Transformer failures in regions incorrectly considered to have low GIC-risk. In Proceedings of the IEEE Lausanne Power Tech. Proceedings, Lausanne, Switzerland, 1–5 July 2007; pp. 807–812.
104. Matandirotya, E.; Cilliers, P.J.; Van Zyl, R.R.; Oyedokun, D.T.; Villiers, J. Differential magnetometer method applied to measurement of geomagnetically induced currents in southern African power networks. *Space Weather.* **2016**, *14*, 221–232. [CrossRef]
105. Liu, C.M.; Liu, L.G.; Pirjola, R.; Wang, Z.Z. Calculation of geomagnetically induced currents in mid- to low-latitude power grids based on the plane wave method: A prelimi-nary case study. *Space Weather* **2009**, *7*, S04005. [CrossRef]
106. Zheng, K.; Liu, L.G.; Ge, H.Y.; Li, W.X. Comparative study of the GIC amplitudes and characteristics in different power grids in China. In Proceedings of the CIGRE Tech. Exhib., Paris, France, 26–31 August 2012. C3–206.
107. Trivedi, N.B.; Vitorello, Í.; Kabata, W.; Dutra, S.L.; Padilha, A.L.; Bologna, M.S.; de Pádua, M.B.; Soares, A.P.; Luz, G.S.; Pinto, F.D.A.; et al. Geomagnetically induced currents in an electric power transmission system at low latitudes in Brazil: A case study. *Space Weather* **2007**, *5*, S04004. [CrossRef]
108. Zawawi, A.A.; Ab Aziz, N.F.; AbKadir, M.Z.A.; Hashim, H.; Mohammed, Z. Evaluation of Geomagnetic Induced Current on 275 kV Power Transformer for a Reliable and Sustaina-ble Power System Operation in Malaysia. *Sustainability* **2020**, *12*, 9225. [CrossRef]
109. Caraballo, R.; SánchezBettucci, L.; Tancredi, G. Geomagnetically induced currents in the Uruguayan high-voltage power grid. *Geophys. J. Int.* **2013**, *195*, 844–853. [CrossRef]
110. Caraballo, R.; González-Esparza, J.A.; Sergeeva, M.; Pacheco, C.R. First GIC estimates for the Mexican power grid. *Space Weather* **2020**, *18*, 2. [CrossRef]
111. Torta, J.M.; Marsal, S.; Quintana, M. Assessing the hazard from geomagnetically induced currents to the entire high-voltage power network in Spain. *Earth Planets Space* **2014**, *66*, 87. [CrossRef]
112. Ribeiro, J.A.; Pinheiro, F.J.G.; Pais, M.A.; Santos, R.; Cardoso, J.; Baltazar-Soares, P.; Monteiro Santos, F.A. Toward more accurate GIC estimations in the Portuguese power network. *Space Weather* **2023**, *21*, e2022SW003397. [CrossRef]
113. Abraha, G.; Yemane, T.; Kassa, T. Geomagnetic storms and their impacts on Ethiopian power grid. *Adv. Astron. Space Phys.* **2020**, *10*, 55–64. [CrossRef]
114. Molinski, T.S. Why utilities respect geomagnetically induced currents. *J. Atmos. Sol.-Terr. Phys.* **2002**, *64*, 1765. [CrossRef]
115. Hughes, J.; Mcgranaghan, R.; Kellerman, A.C.; Bortnik, J.; Arrit, R.F.; Venkataramani, K.; Perry, C.H.; McCormick, J.; Ngwira, C.M.; Cohen, M. Revealing novel connections between space weather and the power grid: Net-work analysis of ground-based magnetometer and Geomagnetically Induced Currents (GIC) measurements. *Space Weather* **2022**, *20*, e2021SW002727. [CrossRef]
116. Zois, J.P. Solar activity and transformer failures in the Greek national electric grid. *J. Space Weather Space Clim.* **2013**, *3*, A32. [CrossRef]
117. Gil, A.; Berendt-Marchel, M.; Modzelewska, R.; Siluszyk, A.; Siluszyk, M.; Wawrzaszek, A.; Wawrzynczak, A. Review of Geomagnetically Induced Current Proxies in Mid-Latitude European Countries. *Energies* **2023**, *16*, 7406. [CrossRef]

118. Výbošt'oková, T.; Švanda, M. Statistical analysis of the correlation between anomalies in the Czech electric power grid and geomagnetic activity. *Space Weather.* **2019**, *17*, 1208–1218. [CrossRef]
119. Gleisner, H.; Thjll, P. Patterns of tropospheric response to solar variability. *Geophys. Res. Lett.* **2003**, *30*, 44-1–44-4. [CrossRef]
120. Gray, G.; Scaife, A.; Mitchell, D.; Osprey, S.; Ineson, I.; Hardiman, S.; Butchart, N.; Knight, J.; Sutton, R.; Kodera, K. A lagged response to the 11 year solar cycle in observed winter Atlantic/European weather patterns. *J. Geophys. Res.* **2013**, *118*, 13405–13420. [CrossRef]
121. Echer, S.; Echer, E.; Rigozo, N.; Brum, C.; Nordeman, D.; Gonzalez, W. The relationship between global, hemispheric and latitudinal averaged air surface temperature (GISS time series) and solar activity. *J. Atmos. Sol.-Terr. Phys.* **2012**, *74*, 87–93. [CrossRef]
122. Maliniemi, V.; Asikainen, T.; Mursula, K.; Seppälä, A. QBO-dependent relation between electron precipitation and wintertime surface temperature. *J. Geophys. Res. Atmos.* **2013**, *118*, 6302–6310. [CrossRef]
123. Christiansen, F.; Haigh, J.D.; Lundstedt, H. Influence of Solar Activity Cycles on Earth's Climate, Final Report, Task 700—Summary Report-Conclusions and Recommendations, ESTEC Contract no. 18453/04/NL/AR, Issue 1. 4 September 2007. Available online: https://www.space.dtu.dk/english/-/media/Institutter/Space/English/reports/scientific_reports/isac_final_report.ashx?la=da&hash=91BA564B50238B03A19F1B11B4BAA8DCC6CA8136 (accessed on 2 October 2023).
124. Ouzounov, D.; Anagnostopoulos, G.C.; Menesidou, S.-A.I.; Karkanis, A.; Efthymiadis, D.A.; Kampatagis, A.; Marhavilas, P.; Danikas, M. Side of a global weather extreme in March 2012, the heat wave in North-East America and the extreme cold weather in South-East Europe as possible effects of intense solar activity. In *AGU Fall Meeting Abstracts; Chicago AGU Fall Meeting 2022*; p. NH14C-05. 2000 Washington, DC 2000. Available online: https://agu.confex.com/agu/fm22/meetingapp.cgi/Paper/1139675 (accessed on 2 October 2023).